

SPECIALLY TREATED GRAPHITE FORTIFIED ALUMINA- SILICON CARBIDE- CARBON REFRACTORIES: FABRICATION AND PROPERTIES

A THESIS SUBMITTED IN PARTIAL FULFILMENT OF THE
REQUIREMENTS FOR THE DEGREE OF

Master of Technology

in

Ceramic Engineering

Submitted by

Kuldeep Singh



Department of Ceramic Engineering

National Institute of technology

Rourkela

2014

SPECIALLY TREATED GREPHITE FORTIFIED ALUMINA- SILICON CARBIDE- CARBON REFRACTORIES: FABRICATION AND PROPERTIES

A THESIS SUBMITTED IN PARTIAL FULFILMENT OF THE
REQUIREMENTS FOR THE DEGREE OF

Master of Technology

in

Ceramic Engineering

Submitted by

Kuldeep Singh

Under the supervision of

Dr. Shantanu Kumar Behera

and

Dr. Sukumar Adak



Department of Ceramic Engineering

National Institute of technology

Rourkela

2014



National Institute of Technology, Rourkela

CERTIFICATE

This is to certify that the thesis entitled, “**Specially Treated Graphite Fortified Alumina-Silicon Carbide-Carbon Refractories :Fabrication and Properties**” submitted by **Mr. Kuldeep Singh** in partial fulfillments of the requirements for the award of master of technology degree in ceramic engineering at National Institute of Technology, Rourkela is an authentic work carried out by him under our supervision and guidance.

To the best of our knowledge, the matter embodied in the thesis has not been submitted to any other University/ Institute for the award of any Degree or Diploma.

Dr. Sukumar Adak
Vice President (Technology)
TRL Krosaki Refractories Ltd
Belpahar
Odisha-768 218

Dr. Shantanu Kumar Behera
Assistant Professor
Department of Ceramic Engineering
Rourkela
Odisha-769 008

Date:

Contents

	Page no.
Abstract	i
Acknowledgements	ii
List of Figures	iii-vii
List of Tables	viii
Chapter 1 Introduction	1-8
1.1 Introduction	2
1.2 Al ₂ O ₃ –SiC–C (ASC) Refractory System	4
1.3 Application of ASC refractory	7
Chapter 2 Literature Review	9-21
2.1 Historical perspectives ASC refractory	10
2.2 With the help of various Carbon Source for improvement of high temperature properties of Graphite based Refractories	12
2.2.1 Use of nano carbon and carbon black	12
2.2.2 Use of Multi-Walled Carbon nanotubes (MWCNTs) and Ultrafine Micro Crystalline Graphite (UMCG) Powders	13
2.2.3 Use of Graphite Oxide, Graphene Oxide Nanosheets (GONs) and Expanded Graphite	14
2.3 Raw materials for ASC refractory	15
2.3.1 Alumina	15
2.3.2 Graphite	17
2.3.3 Resin	19
2.3.4 Antioxidants	20
2.3.5 Silicon Carbide	20

2.4 Special techniques for Exfoliation of graphite	21
Chapter 3 Objective of the work and Special Treated Graphite (STG)	23-24
3.1 Objective of the present work	24
Chapter 4 Experimental Work	25-42
4.1 Raw materials	26
4.2 Preparation of Special Treated Graphite (STG)	28
4.3 Fabrication of ASC brick	29
4.3.1 Batch preparation	29
4.3.2 Mixing	34
4.3.3 Aging	35
4.3.4 Pressing	35
4.3.5 Tempering	35
4.3.6 Coking	36
4.4 Characterizations and measurement techniques	36
4.4.1 Phase analysis	36
4.4.2 TGA analysis	36
4.4.3 Micro-structural analysis of the composite by SEM	37
4.4.4 Apparent porosity (AP) and bulk density (BD)	37
4.4.5 Cold crushing strength (CCS)	38
4.4.6 Hot modulus of rupture (HMOR)	39
4.4.7 Oxidation resistance	40
4.4.8 Thermal shock resistance	41
4.4.9 Static slag corrosion test	41
4.4.10 Permanent Linear change (PLC) on reheating	42

Chapter 5 Results and Discussion-I Effect of STG amount on ASC

Refractories	43-64
5.1 Structure and chemistry of graphite and STG	44
5.2 Effect of STG amount on ASC Refractories	49
5.2.1 Physical properties before coking	49
5.2.2 Physical properties after coking	52
5.2.3 Hot modulus of rupture	55
5.2.4 Thermal shock resistance	57
5.2.5 Oxidation resistance	60
5.2.6 Corrosion resistance	62
5.2.7 Permanent Linear Change (PLC)	64

Chapter 6 Results and Discussion-II Effect of STG/Al₂O₃ mixture ratio on ASC

Refractories	65-73
6.1 Physical Properties (Before Coking)	66
6.2 Physical Properties (After Coking)	68
6.3 Thermal shock resistance	70
6.4 Oxidation resistance	71
6.5 Corrosion resistance	72

Chapter 7 Results and Discussion-III Effect of the type of Alumina fines on ASC

Refractories	74-82
7.1 Physical Properties (Before Coking)	75
7.2 Physical Properties (After Coking)	77
7.3 Thermal shock resistance	79
7.4 Oxidation resistance	80
7.5 Corrosion resistance	81

Chapter 8 Results and Discussion-IV Effect of antioxidant type and amount on

ASC Refractories	83-91
8.1 Physical Properties (Before Coking)	84
8.2 Physical Properties (After Coking)	86
8.3 Thermal shock resistance	88
8.4 Oxidation resistance	89
8.5 Corrosion resistance	90
Chapter 9 Summary and Conclusions	92-95
Scope of future work	
References	96-105

ABSTRACT

In this study, a different method has been followed to increase the thermo mechanical properties and oxidation resistance of Al_2O_3 -SiC-C refractories. In the present work, a specially treated graphite was used as carbon source to partially replace flaky graphite in Al_2O_3 -SiC-C refractories in order to study the effect of its addition on the microstructure and mechanical and thermo-mechanical properties.

Al_2O_3 -SiC-C refractory batches fortified with various fractions of STG were prepared on a pilot plant scale, and their thermo-mechanical properties were studied. Bulk density, apparent porosity, cold crushing strength (of tempered as well as coked specimens), hot modulus of rupture, oxidation resistance, slag corrosion test, permanent linear change and thermal shock resistance were the properties studied across a series of batches. The new compositions exhibited excellent hot strength, thermal shock resistance, slag corrosion resistance and oxidation resistance.

Keywords: Al_2O_3 -SiC-C refractories, specially treated graphite (STG), low carbon Al_2O_3 -SiC-C refractories

ACKNOWLEDGEMENT

With deep regards and profound respect, I avail this opportunity to express my deep sense of gratitude and indebtedness to Prof. Shantanu Behera, Department of Ceramic Engineering, NIT Rourkela, for his inspiring guidance, constructive criticism and valuable suggestion throughout in this research work. It would have not been possible for me to bring out this thesis without his help and constant encouragement.

I would like to express my deepest sense of gratitude to Prof. Swadesh Kumar Pratihari, HOD, Department of Ceramic Engineering, NIT Rourkela for his keen interest, encouragement, constructive suggestions, and esteemed guidance throughout the one year project of this work.

I should also thank Dr S. Adak, Vice President, Technology, TRL Krosaki Refractories Ltd. for permitting me to carry out the major part of my work at the premises of his esteemed company. Another important person who deserves mention is my mentor at TRL Krosaki Refractories Ltd., Dr. M. Sathiyakumar. It was because of his constant guidance and the fact that he always managed quality time for me inspite of his hectic schedule that I was able to complete my project work on time.

I would also like to thank each and every employee at the R&D facility of TRL Krosaki Refractories Ltd. who went out of their way to help me with my work especially Tapas Bhaiya, Ranojit Sir, Rajesh Sir and Debarati Mam.

I would like to express my gratitude to all the faculties of the Department of Ceramic Engineering for their valuable suggestions and encouragements at various stages of the work.

I am thankful to all non-teaching staffs of the Department of Ceramic Engineering for providing all joyful environments in the lab and helping me throughout this project. I am also thankful to research scholars and my classmates in Department of Ceramic Engineering for providing all joyful environments in the lab and helping me throughout this project.

I want to express thanks to my senior Mr. Subham Mahato for his important suggestions and guidance.

Last but not least, my sincere thanks to all my family members and friends who have patiently extended all sorts of help for accomplishing this undertaking.

Date:

Kuldeep Singh

FIGURE NO.	FIGURE DESCRIPTION	Page No.
2.1	Crystal structure of graphite	18
4.1	Flow chart of preparation of STG	28
4.2	Schematic diagram of CCS	39
5.1	SEM images of natural graphite	44
5.2	X-ray diffraction of graphite	45
5.3	Thermal analysis of the natural flake graphite (94FC) sample	46
5.4	FESEM images of STG	46
5.5	X-ray diffraction pattern of STG	47
5.6	Thermal analysis of the STG	48
5.7	Variation of apparent porosity with the variation of STG content	49
5.8	Variation of bulk density with the variation of STG content	50
5.9	Variation of cold crushing strength with the variation of STG content	51
5.10	Variation in coked apparent porosity with the variation of STG content	52
5.11	Variation of coked bulk density with the variation of STG content	53
5.12	Variation of coked cold crushing strength with the variation of STG content	54
5.13	Variation of hot modulus of rupture with the variation of STG content	55
5.14	FESEM images of 1.5 wt. % STG at 1400 °C	56

5.15	Samples after 12th cycle	57
5.16	Samples after 13th cycle	57
5.17	Samples after 14th cycle	57
5.18	Samples after 15th cycle	58
5.19	Sample after 16th cycle	58
5.20	Graph of thermal shock resistance	58
5.21	Images of the cross-section of the ASC specimens with 0%, 1%, 1.5%, 1.75% and 2 % addition of the STG and oxidized at 1400°C for 10 hours	59
5.22	Oxidation Index (%) of tempered ASC samples with 0%, 1%, 1.5%, 1.75% and 2% addition of the STG and oxidized at 1400°C for 10 hours	60
5.23	FESEM images of 0 wt. % STG after oxidation	60
5.24	FESEM images of 1.5 wt. % STG after oxidation	61
5.25	Corroded samples before cutting	62
5.26	Corroded samples after cutting	62
5.27	Graph of penetration depth of Static slag corrosion test	63
5.28	Graph of Permanent Linear Change (PLC %) test	63
6.1	Variation of apparent porosity with the variation of STG/Al ₂ O ₃ mixture ratio	64
6.2	Variation of Bulk Density with the variation of STG/Al ₂ O ₃ mixture ratio	66
6.3	Variation of cold crushing strength with the variation of STG/Al ₂ O ₃ mixture ratio	67
		67

6.4	Variation of apparent porosity with the variation of STG/Al ₂ O ₃ mixture ratio	68
6.5	Variation of Coked Bulk Density with the variation of STG/Al ₂ O ₃ mixture ratio	69
6.6	Variation of Coked cold crushing strength with the variation of STG/Al ₂ O ₃ mixture ratio	69
6.7	Samples after 13th cycle	70
6.8	Graph of thermal shock resistance with the variation of STG/Al ₂ O ₃ mixture ratio	70
6.9	Images of the cross-section of the ASC specimens of Batch 6 oxidized at1400°C for 10 hours	71
6.10	Oxidation Index (%) of tempered ASC Batch 3 and Batch 6 samples oxidized at1400°C for 10hours with the variation of STG/Al ₂ O ₃ mixture ratio	
6.11	Corroded sample of Batch 6 after cutting	71
6.12	Graph of penetration depth of Static slag corrosion test with the variation of STG/Al ₂ O ₃ mixture ratio	72
7.1	Variation of apparent porosity with the different alumina fines	73
7.2	Variation of Bulk density with the different alumina fines	75
7.3	Variation of cold crushing strength with the different alumina fines	76
7.4	Variation of apparent porosity with the different alumina fines	76
		77

7.5	Variation of Bulk density with the different alumina fines	78
7.6	Variation of Coked cold crushing strength with the different alumina fines	78
7.7	Graph of thermal shock resistance with the different alumina fines	79
7.8	Images of the cross-section of the ASC specimens of Batch 7 oxidized at 1400°C for 10 hours	
7.9	Oxidation Index (%) of tempered ASC Batch 3 and Batch 7 samples oxidized at 1400°C for 10 hours with the different alumina fines	80
7.10	Corroded sample of Batch 7 after cutting	80
7.11	Graph of penetration depth of Static slag corrosion test with the different	81
8.1	Variation of apparent porosity with the different antioxidant type	84
8.2	Variation of Bulk density with the different antioxidant type	85
8.3	Variation of Cold crushing strength with the different antioxidant type	85
8.4	Variation apparent porosity of with the different antioxidant type	86
8.5	Variation of Bulk density with the different antioxidant type	87
8.6	Variation of Cold crushing strength with the different antioxidant type	87
8.7	Samples after 14th cycle	88
8.8	Graph of thermal shock resistance with the different antioxidant type	88
8.9	Images of the cross-section of the ASC specimens of Batch 8 oxidized at 1400°C for 10 hours	89

8.10	Oxidation Index (%) of tempered ASC Batch 3 and Batch 8 samples oxidized at 1400°C for 10 hours with the different antioxidant type	89
8.11	Corroded sample of Batch 8 after cutting	90
8.12	Graph of penetration depth of Static slag corrosion test with the different antioxidant type	91

List of Tables:	Page no
Table.4.1: Chemical Analysis of BFA, WTA, Andalusite and reactive alumina:	27
Table.4.2: Chemical analysis of 94 flake graphite:	27
Table.4.3: Physicochemical Parameters of liquid resin:	27
Table.4.4: Purity of Silicon Carbide:	27
Table 4.5: Composition of different batches of ASC bricks prepared in this study	30
Table 4.6: Composition of batch 6 of ASC brick prepared in this study	31
Table 4.7: Composition of batch 7 of ASC brick prepared in this study	32
Table 4.8: Composition of batch 8 of ASC brick prepared in this study	33
Table.4.9: Mixing sequence of ASC bricks	34
Table.4.10: Chemical composition (wt. %) and basicity of the steel making Blast Furnace slag	42

Chapter – 1

Introduction

1.1 Introduction:

Refractories are non-metallic inorganic materials, they have high softening temperature. They also possess good mechanical properties particularly at high temperatures and most often at room temperature as well, good stability on rapid temperature change etc. The materials also have good corrosion and erosion resistance to molten slag, metals and hot gases. According to ASTM C71 “nonmetallic materials having those chemical and physical properties that make them applicable for structures or as mechanisms of systems that are showing to environments above 538°C” [1] Refractories show good mechanical properties at high temperature and as well as at low temperature. They have better corrosion and erosion resistance to molten slag, metals and hot gases. Due to good thermo-mechanical and thermo-chemical properties refractory materials are used in various high temperature processes, including iron and steel making, non-ferrous metal processing, cement, glass, chemical industries, in high temperature furnaces, kilns, boilers and incinerators.

Many of the scientific and technological developments would not have been possible without refractory materials. Manufacturing of any metal without the use of refractory is impossible. Refractories consumption in steel and iron industries is nearly 70% of total refractories production. [2] Iron and steel industries are the highest consumers of refractories. So, the refractory production has to be in sync with the demand of iron and steel industries. Better manufacturing and application environment is challenging a new generation of refractory material with improved properties, performance and life with eco-friendliness.

Refractories can be classified into three major groups based on their constituent phases:-

- a) Acidic (silica, fireclay and zirconia)
- b) Basic (magnesite, magnesia-carbon, alumina/magnesia-carbon, chrome-magnesite and magnesite-chrome, dolomite)
- c) Neutral (alumina, chromites, silicon carbide, carbon and mullite)

Iron and steel industries are the main consumer of refractories. India has appeared as the fourth largest steel manufacturing nation in the world, as per the current figures release by the World Steel Association in April 2011. Total crude steel production in India was around 69 million tons for 2010-2011 and it is expected that the crude steel production capacity in the country will increase day by day. Further, if the proposed expansion plans are completed as per schedule, India is on the way to become the second largest crude steel producer in the world by 2015-16. ^[3] As production of crude steel is increasing at a momentous speed, the production of refractory has also increased over the years to meet the growing demand. Besides, there has been a phenomenal change in refractory technology to fulfill the demand of high quality and quantity steel production. In this situation, carbon containing refractories has found the widest applicability in basic oxygen furnace (BOF), electric arc furnace (EAF) and also in ladle metallurgy due to their good thermal shock resistance and excellent slag-corrosion resistance.

It is well known that the steel metallurgy industries need to consume large amounts of refractory material, including shaped and unshaped refractories. ^[4-6] This is, especially so in puddle blast furnace systems ^[7], with the process engineering of blast furnace shells, casting houses, and molten iron storage, and transportation, etc. ^[8, 9] These require many $\text{Al}_2\text{O}_3\text{-SiC-C}$ (ASC)

refractories. ^[10] Carbon containing refractories have been broadly used as high duty and useful refractories in the metallurgical industry due to their excellent mechanical, thermal and chemical properties. ^[11, 12] Carbon plays an important role in this type of refractories due to its low wettability with molten slag and high thermal conductivity. ^[13,14] Another important benefit of adding carbon is that it reacts with Al or Si additive to form such ceramic phases as Al_4C_3 , SiC , $\text{Al}_4\text{O}_4\text{C}$ and Al_4SiC_4 , which function as strengthening and toughening phases that improve mechanical properties. ^[15, 16] Day by day the production of clean steel calls for developing low carbon technology in refractories increasingly. However, it is sure to deteriorate properties of carbon containing refractories when reducing carbon content simply. For applying low carbon technology in refractories, traditionally, the mixture of different carbon sources, ^[17] such as graphite flake, carbon black, or derivative carbon pyrolyzed from phenolic resin, was added into refractories.

1.2 Al_2O_3 –SiC–C (ASC) Refractory System:

ASC brick is a composite material based on alumina and C and bonded with high carbon containing pitch and resin, with some metallic powder as anti-oxidants to protect the carbon. ASC bricks are made by high pressure. These bricks show excellent resistance to thermal shock and slag corrosion at higher temperatures. ASC bricks are used extensively in steel making processes especially in basic oxygen furnaces, electric arc furnaces, lining of steel ladles, and mostly used in torpedo ladles etc. ^[18]

Some of the important features of ASC refractories are outlined as follows:

1. ASC refractories have high refractoriness as no low melting phase occurs between Al_2O_3 and C.
2. Graphite, the carbon source, has very low thermal expansion; hence in the composite of Al_2O_3 -SiC-C the thermal expansion is generally low.
3. Graphite has very high thermal conductivity, which imparts high thermal conductivity in the Al_2O_3 -SiC-C composites.
4. Thermal shock resistance of ASC is very high because the thermal expansion is low and the thermal conductivity is high.
5. ASC bricks prevent the penetration of slag and molten steel because of the non-wettability of carbon, similar to other graphite based refractories.
6. Better ability to absorb stress, thus keeping down the amount of irregular wear due to cracks.
7. Better spalling resistance, owing to high hot strength of the refractory composite.

ASC bricks consist of alumina, silicon carbide, graphite, antioxidant and binder. Alumina grains are the main constituent of the system which gives very high resistance to basic slag corrosion. Graphite has non-wetting nature which improves the corrosion and thermal shock resistance of the ASC system. However, graphite is liable to oxidation. Antioxidants prevent oxidation of carbon and improve high temperature strength by the formation of various carbides. The carbonaceous binder keeps the different components of the refractory together, which form amorphous carbon after the coking process during which volatile species leave the resin.

ASC refractories have found the widest applicability in BOF and EAF furnaces and also in steel ladle due to their good thermal shock resistance and excellent slag-corrosion resistance at elevated temperature. These properties come due to the non-wetting nature (graphite) with slag, high thermal conductivity and low thermal expansion of carbon. The penetration and corrosion resistance are improved by the formation of a nascent dense layer of Al_2O_3 on the working surface of ASC brick, due to oxidation of Al_2O_3 (produced in the reaction between Al_2O_3 and C). But carbon suffers from poor oxidation resistance and may oxidize to form CO and CO_2 resulting in a porous structure with poor strength and corrosion resistance. Prevention of carbon oxidation is done by using antioxidants, which reacts with incoming oxygen, gets oxidized and protects carbon, thus retaining the brick structure and properties. In presence of high carbon content, conductivity of ASC brick increases and results in loss of heat energy through the furnace wall. Presence of large quantities of carbon in ASC brick makes the reduction of carbon content in steel difficult. Finally the main problem for nowadays is environmental pollution because the higher amount of carbon produces the higher amount of CO and CO_2 which is released into the atmosphere. So the global aim is to reduce carbon content in ASC refractories while retaining the thermo-mechanical properties.

Lot of efforts has been made to develop low carbon refractories for the production of low carbon and ultra-low carbon steels. Approaches used to prepare low carbon refractories with superb mechanical and thermal properties included the addition of micro-/nano-powders and the combination of one dimensional nanosized carbon. For example, carbon black has been used widely in recent years to make low carbon containing refractories. [19–29] Bag et al. [30] reported that the addition of 0.9wt% nano sized carbon in combination with 3wt% flaky graphite gave the best properties in their low carbon MgO-C refractories. Carbon nano fibers (CNFs) or carbon

nano tubes (CNTs) have also been examined for their use as carbon sources for low carbon refractories due to their unique thermal, mechanical and chemical properties. Min Feng Yu et al. reported that tensile strength was increased with the CNFs and CNTs.^[31, 32] Matsuo et al. ^[33] reported an improvement of 2.2 times in strength for the MgO–C specimen containing 0.4wt% CNFs compared to that containing no CNFs, owing to the crack arresting effect of CNFs. Also, Luo et al. ^[34] observed that better mechanical properties can be obtained in Al₂O₃–C refractories when 0.05 wt% CNTs was added. Rountos and Aneziris ^[35] also informed that adding of CNTs in combination with aluminum- nano sheets in Al₂O₃–C refractories led to superior thermal shock resistance. Recently, another new type of nano sized carbon, graphene or graphite oxide nano sheets (GONs), was studied for use as a reinforced phase for the polymer matrix and ceramic matrix composite sowing to its excellent mechanical, thermal and electrochemical properties. ^[36–40] For example, Wang et al. ^[41] obtained a fracture toughness value of 5.21 MPa m^{1/2} for the graphene nanosheets/alumina composites, which was 53% higher than the pure alumina (3.40 MPa m^{1/2}). In the present work, special treated graphite (STG) was used as a carbon source to partially replace flaky graphite in ASC refractories in order to study the effect of its addition on the microstructure and mechanical and thermo-mechanical properties.

1.3 Application of ASC refractory:

Torpedo ladles are usually used for transporting hot metal from blast furnace to steel making shop. Also primary transportation, torpedo cars are also used as iron purification unit and various pretreatments. The operating conditions prevailing in the charge pad, metal and slag zone, mouth areas of torpedo ladles vary significantly.

ASC bricks used in:

- Melting iron pretreating equipment
- Work lining of Torpedo ladles
- Work lining of hot metal transfer ladles
- Used as the tailing bricks of steel tapping hole
- Steel tapping hole of EAF
- Used as transfer ladles

ASC refractory is one of the highest consumable refractory items in steel sector. The demand of steel in the country is currently growing at the rate of over 8% and it is expected that the demand would grow over by 10% in the next five years. So it is expected that demand of ASC refractories will also increase with the demand of steel. Selection of raw materials, their grading and grain size distribution and composition play a very important role in the development of various physical properties, microstructure and thermo-mechanical properties of ASC refractory bricks. Various different types of Al_2O_3 (alumina) grains provide different levels of corrosion resistance. Because of its unique advantages and very high demand in steel industry there is a huge scope and requirement of further improvement in the properties of ASC refractories.

Chapter – 2

Literature Review

2.1 Historical perspectives ASC refractory:

Carbon has been accepted as a very important component of refractories after 1950's. The addition of carbon results to a better thermal and chemical resistance and hence the life of refractory linings has been increased, which ultimately reduces the cost of steel production. [42, 43] Nowadays carbon containing refractories have been recognized for many different applications. As described by Sidinei N Silva et al [44] high alumina bricks were generally used in the torpedo ladle because of its compatibility with the acidic slag along with the hot metal transportation. But due to the formation of eutectic phase at lower temperature and to have better thermo-mechanical stress later on ASC bricks have been effectively used in charge pad and slag line area of torpedo ladle. [45-46] In recent years, with the development of blast furnace melting technology, melting intensity continues to increase, in 2011 the country has reached the blast furnace pig iron 628 million tons, consumption of blast furnace refractories larger. Al_2O_3 -SiC-C castable with high strength, erosion resistance, thermal shock resistance and long life and other characteristics, both carbon and silicon carbide, high thermal conductivity, low expansion and slag are given this non-wetting material system good physical and chemical properties, which are widely used in blast furnace. In present invention aims to overcome the existing technical defects, the purpose is to provide a simple process for lightweight Al_2O_3 -SiC-C refractory castable preparation, prepared by the method of light Al_2O_3 -SiC-C castable not only high strength, excellent thermal shock resistance, anti-erosion ability and medium low thermal conductivity, and the apparent porosity and pore size controllable; ditch the article for the iron, torpedo car, Mixer and ladle (tank). The carbon has low wettability and excellent thermal shock resistance at operating temperature therefore the slag does not get wet and the service life of the ASC brick increases.

However, the carbon has poor oxidation resistance as one of the drawback thus higher carbon content in ASC refractory tends to oxidize at higher temperatures. After the oxidation of carbon, the structure of ASC brick is destroyed and the slag can penetrate into the structure. Due to this problem the brick lining gets eroded and the brick loses its strength. To reducing this problem, several additives such as antioxidants are usually added to the refractory batches during brick fabrication .Antioxidants often used in ASC refractories include metals/alloys (such as aluminum metal powder).^[47]

Masaaki Mishima et al.^[48] have studied the effect of varying the carbon content of the ASC brick on the shell temperature of torpedo cars, which is very critical for the operation of the torpedo. Torpedo car linings have undergone important changes over the years.^[49-51] The main reasons were severe working condition in blast furnace area i.e. increasing temperature, desulphurization and other metallurgical treatments. Wang Zhanmin et al.^[52] reported that the addition of different metal additives not only affects the oxidation behavior of ASC system but also has an effect on the sintering behavior of the refractories on the service condition. Liu Guoki et al^[53] studied the mutual effect of addition of different metallic additives in the alumina – carbon system. The bonding phases as well as the properties (especially thermo mechanical properties) of the ASC system were found to improve extremely by the addition of these additives. $\text{Al}_2\text{O}_3\text{-SiC-SiO}_2$ composites have been widely used as high duty and functional castable refractories in numerous applications in the iron and steel making industry especially in blast furnace iron/slag runners due to their excellent mechanical, thermal and chemical properties.^[54] Carbon plays an important role in these type of refractories owing to its low wettability with molten slag and high thermal conductivity.^[55] $\text{Al}_2\text{O}_3\text{-SiO}_2\text{-SiC-C}$ resin bonded composites form an important type of new composites for such iron making applications as iron

and slag runners in blast furnaces, furnace bottom, and electric-furnace spouts.^[56] They can be changed from high performance chamotte–carbon and bauxite–carbon composites. This type of composites shows not only superior slag corrosion and erosion (wear) resistance, but also excellent thermal shock resistance and mechanical properties. These composites contain mainly of aluminosilicate and carbon bonds formed by carbonization of phenol resins (resole) during firing of the composite. ^[56-57] V. Roungos and C.G. Aneziris reported that thermal shock of Al_2O_3 –C refractories was improved by the nanoscaled additives. Magnesium aluminate spinel (MgAl_2O_4), alumina nanosheets ($\alpha\text{-Al}_2\text{O}_3$) and carbon nanotubes (CNTs) were used as nano scaled additives. It was found out by the study that overall best properties were performed by the alumina nano sheets and carbon nano tubes. ^[58]

2.2 With the help of various Carbon Source for improvement of high temperature properties of Graphite based Refractories:

2.2.1 Use of nano carbon and carbon black:

Recent research has discovered that replacing graphite flakes with nano carbon powder can induce in situ formation of nano fibres in the matrix of C-containing refractories, which can improve the refractories properties and performance. With the addition of nano carbon and carbon black thermal shock resistance, heat and oxidation resistance were improved. ^[59-60] Now a days the production of clean steel calls for emerging low carbon technology in refractories increasingly. It is bound to deteriorate properties of carbon containing refractories if carbon content is simply reduced. In general, the mixture powder of carbon sources, such as graphite flake, carbon black, or derived carbon from phenolic resin, is added into low carbon containing refractories.^[61] In that case it is difficult to separate the effect of each carbon source on the

morphologies of in-situ formed ceramic phases most important to the blindness for further optimizing mechanical properties. Actually, morphologies of strengthening phases affect mechanical properties of composite materials, no matter whether they are introduced as a metal, or ceramic. It was informed that different carbon sources can be used to synthesize SiC of different morphologies ^[62-63] which will construct the microstructures and increase their properties of materials. ^[64-65]

2.2.2 Use of Multi-Walled Carbon nanotubes (MWCNTs) and Ultrafine Micro Crystalline Graphite (UMCG) Powders:

Another study reported that microstructures and mechanical properties of Al₂O₃-C refractories with Al, Si and SiO₂ as the additives fired in the temperature range from 800 to 1400 °C were investigated, when multi-walled carbon nanotubes (MWCNT) were used as the carbon source to partially or totally replace graphite flake in the materials. The results showed that specimens with only graphite flake, specimens containing 0.05 wt. % MWCNTs possessed better mechanical properties at further increased of MWCNTs amount from 0.1 to 1 wt. % properties deteriorated. The Cold modulus of rupture (CMOR) and flexural modulus (E) values are 23.70 MPa for CMOR and 3733.36 for E, secondly 14.11 MPa for CMOR and 2540.91 for E were reported at 1200 °C for 0.05% and 0% MWCNTs. ^[66] A recent study addition of ultrafine micro crystalline graphite (UMCG) powders in Al₂O₃-C refractory showed that microstructure and mechanical properties were improved with the addition of UMCG in comparison to the graphite. ^[67]

2.2.3 Use of Graphite Oxide, Graphene Oxide Nanosheets (GONs) and Expanded Graphite:

Wang et al. reported that mechanical properties such as cold modulus of rupture (CMOR), flexural modulus (E), force and displacement curves of $\text{Al}_2\text{O}_3\text{--C}$ refractories with graphene oxide nano sheets (GONs) were improved in comparison with those without GONs. They reported that CMOR and E value increased with increasing expanded graphite amount at a certain amount after that, values were decreased. The highest value of CMOR and E was found with 0.21% of expanded graphite. CMOR and E value at 1200 °C for 0.21% were 25.60 MPa and 3.48 GPa and for 0% expanded graphite values were 17.16 MPa for CMOR and 2.87 GPa for E. [68]

Graphite has very high thermal conductivity. So, energy loss is greater for ASC bricks. In order to reduce the energy consumption due to loss of heat, it is preferred to have relatively low carbon content in ASC refractories. But, this leads to lower thermal shock resistance. In recent years, the reduction of carbon content in ASC refractories is the main aim of the research. Extensive research is ongoing to reduce the carbon content of ASC refractories without deterioration of its properties.

2.3 Raw materials for ASC refractory:

The raw materials play a dynamic role in the performance and life of the refractories. Different alumina aggregates, in general fused and sintered alumina have been used for the processing of the ASC refractories. White fused alumina (WFA) and brown fused alumina (BFA) are classified under the fused alumina category and tabular alumina (TA) is under sintered category. The main raw materials are alumina, silicon carbide, graphite; antioxidants and binder, including pitch powder and resin. Details of the each of the raw materials are described below.

2.3.1 Alumina:

Alumina is the main constituent of ASC brick which contains about 83 wt. % or more of the total batch. Three different types of alumina raw materials are used to produce ASC brick.

- i. Brown fused alumina (BFA)
- ii. White tabular alumina(WTA)
- iii. Andalusite
- iv. Calcined alumina
- v. Reactive alumina

Andalusite:

Three specific properties of andalusite are very interesting for the production of high-quality refractories, that andalusite is free of water; its crystal remains stable without changing its density or volume after firing and therefore has no internal porosity and low thermal conductivity.

Calcined alumina: Properties of calcined alumina are

- Enhanced refractoriness and performance
- Improved mechanical strength
- High abrasion resistance
- Thermal shock resistance

Reactive alumina: Properties of reactive alumina are

- Low open porosity
- Excellent sinter reactivity
- Excellent wear resistance and mechanical strength

General Idea about Alumina Aggregates:

Brown fused alumina (BFA) are basically impure ($\sim 95\% \text{Al}_2\text{O}_3$) but extremely dense material, high abrasion resistance. The tabular alumina is highly chemical pure ($>99\% \text{Al}_2\text{O}_3$) and has high particle density. The materials have excellent volume stability and chemical inertness. Although the total porosity of white fused alumina is parallel to the tabular alumina, it contains mainly large interlocking open micro pores. The crushing strength of white fused alumina is lower than the brown fused alumina and tabular alumina. The porosities in tabular alumina are spherical closed pores only. The open porosity of white fused alumina is three times higher than the tabular alumina. The presence of uniformly distributed closed pores in tabular alumina contributes to the low water absorption. An extreme open porosity would also result in greatly differing grain strength and high temperature volume stability. Partially sintered grains would

show poor volume stability and shrink further when used at high temperature. Although higher density has been found in brown fused alumina, the thermal shock resistance of brown fused alumina reduces due to absence of closed porosity. Due to the presence of TiO_2 , brown fused alumina leads to higher densification. But liquid phase sintering already would appear at higher temperature, which results in degradation of high temperature properties. The thermal spalling resistance of tabular alumina is very high due to the presence of closed porosity. The spherical closed pores act as inhibitor to crack transmission during thermal cycling. ^[69] The rough and irregular shape surface morphology of tabular alumina aggregates offers better interlocking with other aggregates and shows better mechanical strength. But, the fused alumina aggregates grain shows smooth surface resulting lower mechanical strength in comparison to the sintered alumina. ^[70]

2.3.2 Graphite:

Carbon is found in the form of diamonds, graphite and as coal. For refractory purpose natural and artificial graphite are important for manufacturing of carbon bricks. The raw materials for carbon should have ash content as low as possible as well as a high yield. ^[71] The graphite structure is well known ^[72-74] fig. and indicates a planer structure with an infinite two dimensional array of carbon atoms arranged in hexagonal networks in the form of an atomic molecule. The C-C bond (covalent) the plane is strong as indicated by the interatomic distance of 0.142 nm where the bonding (van der Waal type) between the planes is weak the interatomic plane spacing being 0.304 nm.

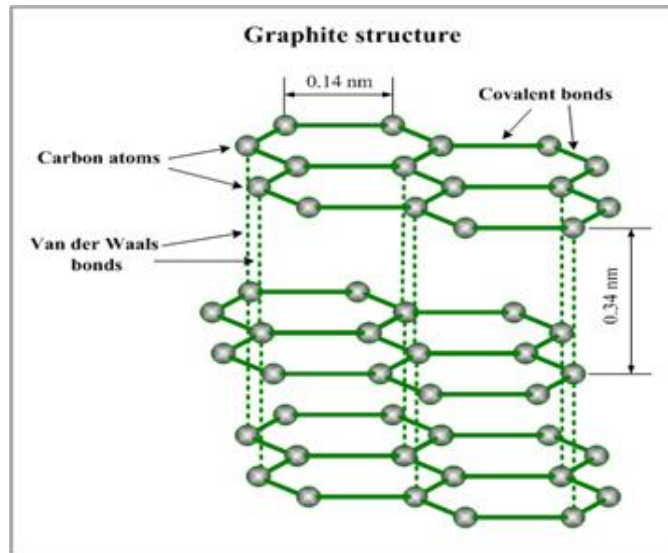


Fig.2.1: Crystal structure of graphite

Flaky graphite is used as a source of carbon in the manufacturing of ASC refractories due to its following properties:-

- High melting temperature
- High thermal conductivity
- Low thermal expansion coefficient
- High thermal shock resistance
- Low friction and hence good compressibility character
- Low wettability to molten slag (because low interfacial tension between graphite and molten materials) and hence better corrosion or erosion resistance
- Bad oxidation resistance. It starts to be oxidized in oxidizing atmosphere at (500 °C)

2.3.3 Resin:

Because of flaky and non-wetting characteristics of graphite, it is very difficult to produce a dense brick without any strong binder. The main role of binder is to provide green strength to ceramic bodies. Resin was found to be the best binder for ASC refractories because of these following properties-

- i. Resin contains high amount of fixed carbon which gives strong bonding property.
- ii. Resin has a high chemical affinity towards graphite and magnesia grain.
- iii. Because of its thermosetting nature resin possesses high dry strength.
- iv. It produces less hazardous gas than tar/ pitch.
- v. At curing temperature ($\sim 200^{\circ}\text{C}$) resin polymerizes which gives isotropic interlocking structure.
- vi. Cold crushing strength (CCS) increases with the increase of resin content.

The desired viscosity of resin should be around 8000 cps, which ensures proper mixing of the other raw materials. Viscosity of resin is quite sensitive to temperature which increases with decrease in temperature. So, in winter viscosity of resin increases, this causes low dispersion of ingredients in the mixer machine. Whereas in summer, due to high temperature, viscosity decreases which gives less strength in the green body and creates lamination. Powder novalac resin is normally used to overcome this type of difficulty. ^[75] Compressibility during pressing improves with the increase in resin content and consequently the CCS of the tempered samples increase. The resole type resin is best as binder among various resin types. Because of its lower viscosity and lower content of volatile species the samples containing resole had the lowest porosity after heating at high temperature.

2.3.4 Antioxidants:

The antioxidant (usually additives) plays important role in ASC refractories in the context of oxidation protection of carbon bonds. The function of antioxidant is given as below:-

- They themselves melt or form low melting glassy phase and coats the carbon bonds and to protect them from being oxidized.
- Get oxidized and reduce the partial pressure of oxygen available to oxidize the carbon bonds.

However, the addition of antioxidants should be optimized to make a balance between the properties of oxidation and corrosion resistance. Generally, metallic silicon, aluminium powder or a combination of Al and Si powders are used as antioxidants (or additives) in the ASC refractories to improve the physical and thermo-mechanical properties.

2.3.5 Silicon Carbide:

Silicon carbide is a structural material with low density, which can bear high temperature, good resistance to oxidation, wear and creep and possess high strength. Silicon carbide has a high dissociation temperature of about 2600 °C. ^[76] It does not show any congruent melting point. At the dissociation temperature, it decomposes into graphite and molten Si. In an open system silicon carbide decomposes at about 2300 °C, into gaseous silicon and a rest of graphite.

2.4 Special techniques for Exfoliation of graphite:

Exfoliation is mainly done by rapid heating or flash heating of graphite intercalation compounds. Due to the sudden volatilization of intercalate a huge unidirectional expansion occurs. There are several techniques for exfoliation of graphite.

Wen-Shyong Kuo et al. used a mixture of concentrated sulfuric acid and nitric acid (4:1, v/ v) as intercalate agent which was mixed with graphite flakes at room temperature. The reaction mixture was stirred continuously for 16 hrs. The acid-treated natural graphite was washed with water until neutralized and then dried at 100°C to remove remaining water. The dried particles were heat-treated at 1050°C for 15sec to obtain expanded graphite particles with a “c” dimension about 300 times that of the original “c” direction dimension. ^[77]

Zhang Shengtao et al. used potassium permanganate and formic acid to intercalate the graphite together with sulfuric acid and nitric acid. Heating temperature was varied from 800 °C to 900°C. ^[78]

Eduardo H.L. Falcao et al. reported the exfoliation of graphite by microwave heating. Potassium-THF (tetra hydro furan) was used to intercalate the graphite. Graphite and potassium were heated in an evacuated, flame-sealed glass tube to afford KC_8 which was transferred to flasks containing THF. Then it was soaked for 4–24 hrs and sonicated for about 1 hrs. The subsequent black solid was filtered, dried (~70 °C) and transferred to glass tubes which were heated at high power in a commercial MW oven to obtain expanded graphite. ^[79]

A. Yoshida et al. have reported difference in morphology between the exfoliated graphite created by five different intercalation compounds (GICs) with H_2SO_4 , $FeCl_3$ & Na tetra hydro furan

(THF), K-THF and Co-THF from flaky natural graphite powder with the average particle size of 400 μm .^[80]

Beata Tryba et al. have reported that, the exfoliation of two residue compounds with H_2SO_4 under microwave of different powers. The first residue compound was prepared through electro chemical intercalation (anodic oxidation) of H_2SO_4 with an electric power consumption of 7.7 A h/kg, followed by water rinsing and the second residue was prepared through washing the intercalation compound produced in concentrated H_2SO_4 with H_2O_2 at room temperature (chemical intercalation).^[81]

Tong Wei et al. have reported a rapid and better method to prepare exfoliated graphite by microwave irradiation. Unlike previous reported methods, the natural graphite (NG), oxidant (KMnO_4) and intercalation agent (HNO_3) were only simply mixed before MW irradiation, and then put for 60 seconds under in MW irradiation.^[82]

Among all the techniques, MW irradiation is very encouraging, because it can be performed at room temperature in a short time with the consumption of less energy.

Chapter- 3

Objective of the work

3.1 Objective of the present work:

ASC refractory is an important item for steel production which possesses many advantages as a torpedo ladle. But; there are several problems still to be resolved. Therefore huge scope of further research and development still exists in this field. In recent times, the main aim of research is to reduce carbon content in ASC refractories while retaining all the good properties.

Because of good thermal shock resistance and excellent slag-corrosion resistance at elevated temperature ASC bricks have found the widest applicability in BOF and EAF furnaces and also in steel ladle. Graphite fills the pores of ASC brick and improves the non-wetting property of the bricks and there by improves the slag corrosion resistance. But higher amounts of graphite are associated with several difficulties, including high thermal conductivity and relatively low strength particularly at high temperatures. Another area of concern is the environmental pollution due to the produced CO and CO₂ during volatilization oxidation of the resin in ASC bricks.

In this study, different approaches have been followed to reduce the carbon content as well as to increase the thermo-mechanical properties and oxidation resistance. In this study exfoliated graphite has been chosen to partially substitute the graphite phase in ASC refractories. An attempt has been made to produce expanded graphite for use in ASC refractories. Small amounts of exfoliated graphite have been used to partially replace the graphite phase in a conventional ASC brick formulation and a few selected properties have been measured. An important feature of this work is the fabrication of the refractory specimens in plant conditions with characterization and property evaluation being done as with industrial specimens.

Chapter-4

Experimental Work

4.1 Raw materials:

Commercially available high quality with low impurity alumina, natural flakes graphite, aluminum metal powder (- 150 μm), silicon metal powder, silicon carbide (SiC) and expanded graphite were used to maintain the granulometry of the mixture. Al and Si metal powder were used as antioxidants. Liquid resin and powder resin were taken as additives of base raw materials for the fabrication of low carbon graded Al_2O_3 -SiC-C brick.

Different types of alumina which is used in work:

- (a) (BFA)brown fused alumina (3-5)
- (b) BFA(1-3)
- (c) BFA(0-1)
- (d) Andalusite(0-1)
- (e) (WTA)white tabular alumina(-325mesh)
- (f) calcined alumina
- (g) reactive alumina

As mentioned earlier, this research work is centered on the preparation of expanded graphite, to use in ASC refractory as partial replacement of graphite.

The main raw materials used for developing high performance ASC bricks are dense fused alumina grains, silicon carbide, natural graphite, liquid resin and metallic additives. 94 flack graphite (FG) was taken as a raw material for carbon. The chemistry of the BFA, Andalusite, WTA, flake graphite and liquid resin are given in the tables below.

Table.4.1: Chemical Analysis of BFA, WTA, Andalusite and reactive alumina:

Ingredients (wt %)	BFA	Andalusite	WTA	Reactive Alumina
Al₂O₃	95.1	58.8	99.5	99.3
Fe₂O₃	0.47	0.85	0.1	0.1
SiO₂	0.82	40.4	0.1	0.2
TiO₂	2.65	0.15	-	-
Na₂O + K₂O	0.14	0.17	0.15	0.28

Table.4.2: Chemical analysis of 94 flake graphite:

Raw materials	Carbon (%)	Volatile matter (%)	Ash (%)
Flake Graphite	94.1	0.75	5.15

Table.4.3: Physicochemical Parameters of liquid resin:

Properties	Liquid resin
Viscosity (CPS) at 25°C	9800
Specific gravity at 25°C	1.23
Nonvolatile matter (%)	78.88
Fixed carbon (%)	47.80
Moisture (%)	3.30

Table.4.4: Purity of Silicon Carbide:

Raw Material	% SiC	% LOI
Silicon Carbide	95.33	0.18

4.2 Preparation of Special Treated Graphite (STG):

To prepare the STG, the raw materials were used natural flake graphite (94FC), Potassium permanganate (Fisher Scientific, 99.6%) and concentrated nitric acid (65%).

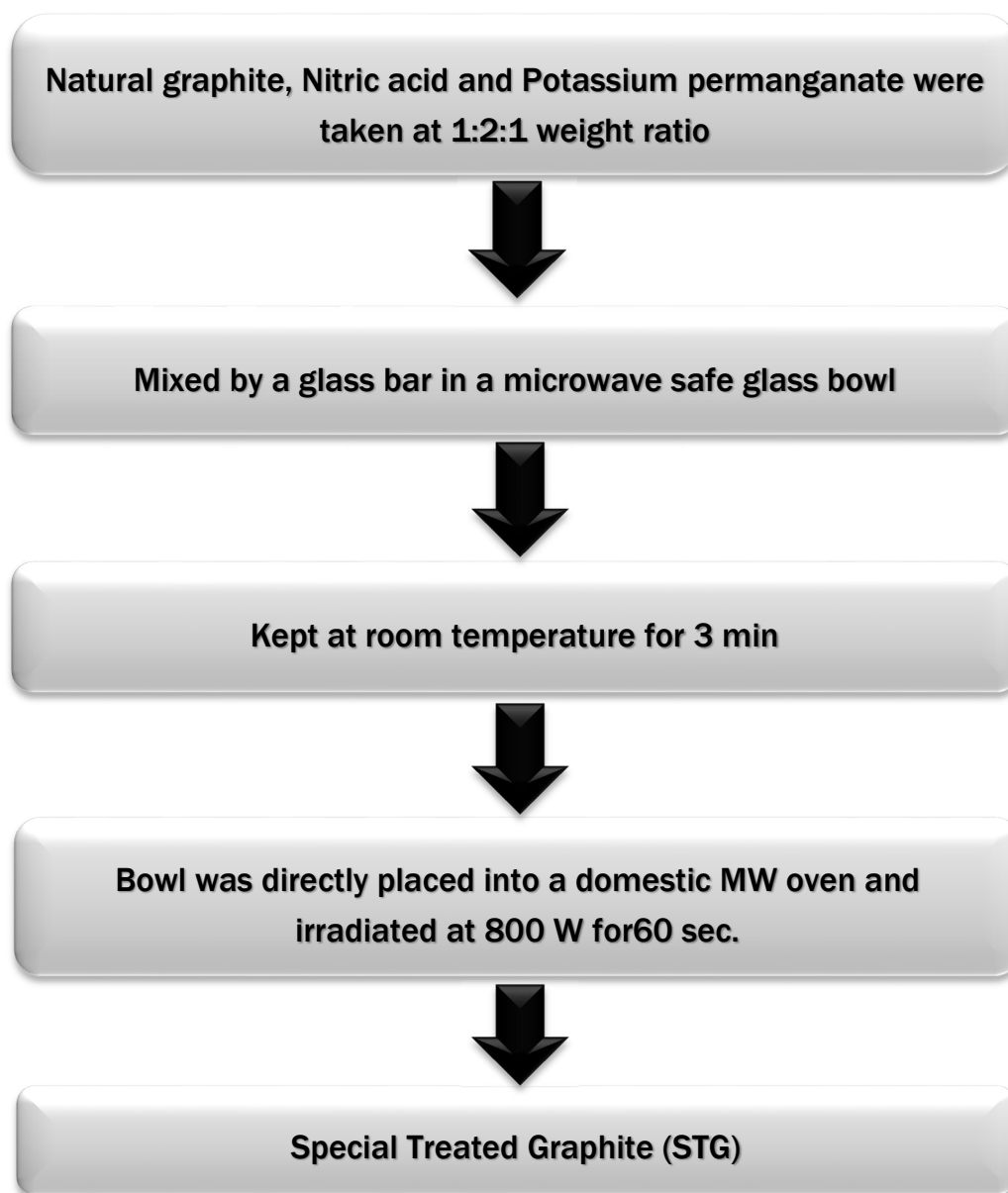


Fig.4.1: Flow chart of preparation of STG

4.3 Fabrication of ASC brick:

The composite material prepared as above, was used to replace a part of the graphite phase for the preparation of a limited number of ASC refractory bricks.

4.3.1 Batch Preparation:

Different batches (batch1 to batch5) of ASC brick were prepared by taking the same amount of alumina, resin and anti-oxidant contents. However, Different compositions of ASC bricks have been fabricated using different amounts of STG as partial replacement of the natural flake graphite. All the batches were prepared in identical conditions. All the variations done in the study are compared with the conventionally used ASC brick composition prepared under similar conditions. Compositions of different batches are given in the following table:

Table 4.5: Composition of different batches of ASC bricks prepared in this study

Ingredients (wt. %)	Batch1	Batch2	Batch3	Batch4	Batch5
BFA(3-5)	5	5	5	5	5
BFA(1-3)	37	37	37	37	37
BFA(0-1)	12.5	12.5	12.5	12.5	12.5
Andalusite(0-1)	13	13	13	13	13
WTA(-325mesh)	5	5	5	5	5
Calcined alumina(2μ)	10	10	10	10	10
94FG	7.5	6.5	6	5.75	5.5
STG	0	1	1.5	1.75	2
SiC(-100mesh)	8	8	8	8	8
Al metal powder	2	2	2	2	2
Liquid resin(Resole)	2.5	2.5	2.5	2.5	2.5
Powder resin	1	1	1	1	1
Pitch powder	1	1	1	1	1

Table 4.6: Composition of batch 6 of ASC brick prepared in this study

Ratio of STG to alumina – (1:2), Alumina fine-Calcined alumina

Ingredients (wt. %)	Batch 6
BFA(1-3)	45
BFA(0-1)	15.5
Andalusite(0-1)	13
WTA(-325mesh)	5
Calcined alumina(2μ)	4
94FG	6
STG	1.5
SiC(-100mesh)	8
Al metal powder	2
Liquid resin(Resole)	2.5
Powder resin	1
Pitch powder	1

Total calcined alumina wt. % in batch6 is 4% and STG is 1.5 wt. %.

Table 4.7: Composition of batch 7 of ASC brick prepared in this study

Ratio of STG to alumina – (1:2), Alumina fine-Reactive alumina

Ingredients (wt. %)	Batch 7
BFA(1-3)	45
BFA(0-1)	15.5
Andalusite(0-1)	13
WTA(-325mesh)	5
Reactive alumina	4
94FG	6
STG	1.5
SiC(-100mesh)	8
Al metal powder	2
Liquid resin(Resole)	2.5
Powder resin	1
Pitch powder	1

Total reactive alumina wt. % in batch7 is 4% and STG is 1.5 wt. %.

Table 4.8: Composition of batch 8 of ASC brick prepared in this study

Ratio of STG to alumina – (1:5), Alumina fine-Calcined alumina

Ingredients (wt. %)	Batch 8
BFA(3-5)	5
BFA(1-3)	37
BFA(0-1)	12.5
Andalusite(0-1)	13
WTA(-325mesh)	5
Calcined alumina(2μ)	10
94FG	6
STG	1.5
SiC(-100mesh)	8
Al metal powder	1
Si metal powder	1
Liquid resin(Resole)	2.5
Powder resin	1
Pitch powder	1

Total calcined alumina wt. % in batch8 is 10% and STG is 1.5 wt. %.

4.3.2 Mixing:

The purpose of mixing is that, the raw materials is to make a refractory batch and transform all the solid components and the liquid additions into a macro homogeneous mixture that can be successively molded or shaped by one of the abundant fabrication methods employed by modern refractory manufacturers. All the above batches were separately mixed in a Hobart mixer at room temperature for a period of 40 minutes. All the solid raw materials and liquid additives are mixed in a sequence for a macro homogeneous mixture.

The following table shows the mixing order of various raw materials.

Table.4.9: Mixing sequence of ASC bricks

Steps	Sequence of mixing	Mixing time (min)
1	BFA(3-5)+BFA(1-3)+Flakes graphite +Al /Si metal powder +Pitch powder	5
2	Liquid resin	15
3	BFA(0-1)+Andalucite(0-1)+WTA+calcined/reactive alumina+SiC+STG	10
4	Powder Resin	10

4.3.3 Aging:

After homogeneously mixing of the materials, the batches were kept for 2 hours for ageing. During aging the polymerization of resin takes place by developing carbon-carbon bonds.

4.3.4 Pressing:

After aging the mixed materials were compacted to give a desired shape by pressing. The aged mixtures were pressed uniaxially by hydraulic press in a steel mold. An appropriate weight of each mixture was taken to get the desired green density and the size of the sample. The steel mold was cleaned using brush and cotton after each pressing. For avoiding stickiness between the mixture and mold, kerosene was used as a lubricating agent. The mixtures were charged slowly into the mold cavity and leveled uniformly in order to escape lamination in the pressed sample. To avoid cavity and for uniformly filling of materials in the mold poking was done during each pressing.

4.3.5 Tempering:

Tempering is the heat treatment process of the refractories at a lower temperature to remove volatile matters from the organic green binders and to give enough green strength for handling. During this process the chemical bond and bonding phases are developed in the refractory grains. Tempering of the pressed green samples was done at 370 °C for 7 hours. With the increase in temperature resole resin got converted to carbonaceous phase which helped in developing a stronger carbonaceous bond for the refractory brick and increased the mechanical strength of the brick.

4.3.6 Coking:

After tempering the bricks were cut into different sizes pieces for the purpose of different testing. Coking was carried out at 1000 °C for 4 hours under reducing atmosphere (carbon bed). Carbon bed was used for preventing to oxidize the samples.

4.4 Characterizations and measurement techniques:

4.4.1 Phase analysis:

Phase analysis of the samples was carried out by standard powder x-ray diffraction technique using Cu K α radiation with a step-scanning speed of 22.7 °/min. Diffraction patterns were analyzed with the help X'pert High Score software. Intensity ratios were calculated from the digital counts for the relevant peak positions (highest peaks of each of the phases).

4.4.2 TGA analysis:

Thermal analysis of the samples was carried out primarily to determine the oxidation temperature of graphite and also to measure the amounts of residue, which has been assumed to the quantity of silicon carbide contained in each of the samples prepared in this investigation. For this purpose, a small quantity of the sample was subjected to TGA analysis in flowing argon atmosphere with a heating rate of 10 °C/minute.

4.4.3 Micro-structural analysis of the composite by SEM:

Microstructures of natural flake graphite, STG were studied using standard NIT RKLNOVA NANO SEM. The accelerating voltage was 10 kV. The powders were fixed on a self-adhesive carbon tape. For micro-structural analysis of ASC samples we cut thin pieces from the bricks. Then those thin slices of samples were coated.

4.4.4 Apparent porosity (AP) and bulk density (BD):

AP is defined as ratio of the total volume of the closed pores to its bulk volume and expressed as a percentage of the bulk volume. Closed porosity is the pores that are not penetrated by the immersion liquid, whereas open porosity are those pores which are penetrated by the immersion liquid. AP was measured as per the standard of IS: 1528, Part-8(1974) both for tampered and coke samples. The Archimedeian evacuation method generally measures both bulk density and apparent porosity.

The test samples were cut from the tempered bricks. After taking dry weight all the samples were put into a container and water was added. Then the container was heated for 2 hrs. So that all the open pores are filled with water. After that, the suspended weight (W_2) and soaked weight (W_3) were taken and AP was calculated as follows:

$$AP = (W_3 - W_1) / (W_3 - W_2) \times 100$$

BD is the ratio of the mass of the dry material of a porous body to its bulk volume expressed in gm/cm^3 or kg/m^3 , where bulk volume is the sum of the volumes of the solid material, the open pores and the closed pores in a porous body. BD was measured as per the standard of IS: 1528, Part -12 (1974) both for tampered and coke samples.

Whereas true density is the ratio of mass of the material of a porous body to its true volume and true volume is the volume of solid material in a porous body.

$$B.D = (W_1/W_3 - W_2) \times \text{density of liquid at temperature of test}$$

(e.g. density of water at 25°C : 0.997044 gm/cc, at 30°C : 0.995646 gm/cc)

4.4.5 Cold crushing strength (CCS):

Cold crushing strength of refractory bricks and shapes is the gross compressive stress required to cause fracture. The cold crushing strength of the tempered and coked samples was measured as per ASTM C-133. Cold crushing strength of the refractories is measured by placing a suitable refractory specimen on a flat surface followed by application of uniform load to it through a bearing block in a standard mechanical or hydraulic compression testing machine (Toni Veral Germany). The load at which crack appears in the refractory specimen represents the cold crushing strength of the specimen. The load is applied uniformly on the sample in the flat position. It is expressed as kg/cm².

The working formula for calculating CCS is given by,

$$CCS = \text{Load/Area (kg/cm}^2\text{)}$$

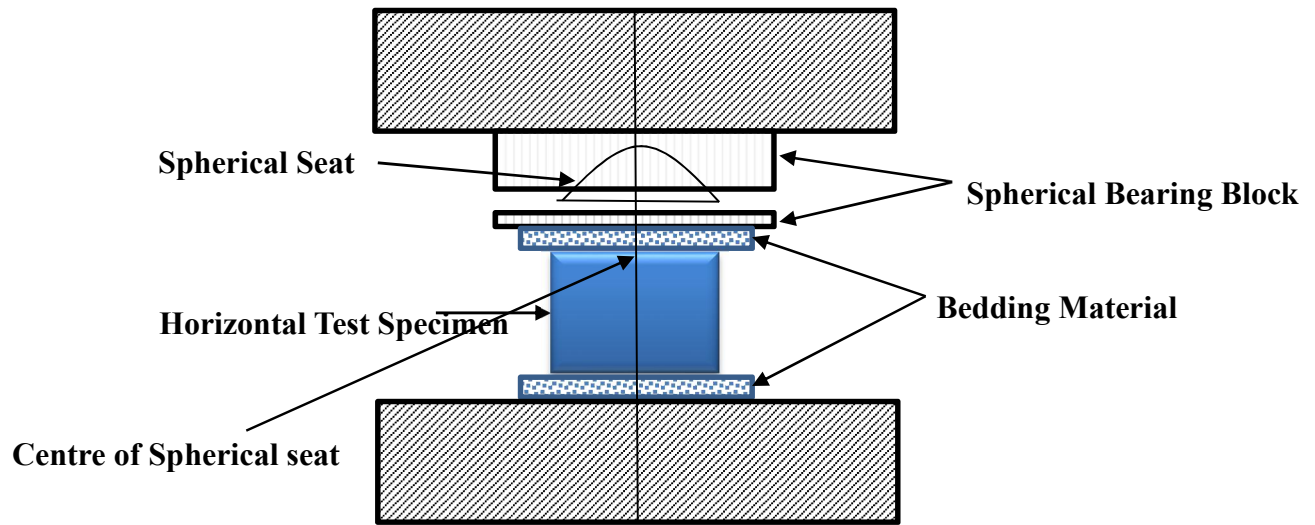


Fig.4.2: Schematic diagram of CCS

4.4.6 Hot modulus of rupture (HMOR):

The modulus of rupture of refractory specimen is determined as the amount of force applied to a rectangular test piece of specific dimensions until failure occurs. This test method covers the determination of the modulus of rupture of carbon-containing refractories at elevated temperatures in air. It was determined as per ASTM C133-7. Each value of HMOR was the average of two parallel specimens. It was done by three - point bending test using HMOR testing apparatus. All the specimens for HMOR were taken as 150mm × 25 mm × 25 mm without pre - firing at air atmosphere. The final temperature of HMOR was 1400 °C with a heating rate of heating rate of 5 °C/min. It was done in air atmosphere with a soaking time of 30 min. Finally, the loading rate of HMOR was 1.2-1.4kg/s according to samples.

The HMOR value was calculated by the following formula:

$$\text{HMOR} = (3 W \times L) / (2 b \times d^2)$$

Where “W” (kg) is the maximum load when the specimen is broken;

“L” is the span length between the lower supporting points. (125 mm for all the tests in the work);

“b” is the breadth (cm), “d” is the height of the specimen(cm).

4.4.7 Oxidation resistance:

The samples were fired in an electrical furnace at 1400 °C for 10 hours in air atmosphere. At this temperature all the carbonaceous materials of the brick got oxidized particularly from the outer surface. The color of the oxidized portion turned off-white compared to the black color of the virgin brick and therefore the boundary between the un-oxidized and the oxidized regions were quite evident. After the heat-treatment, the cuboid shaped samples were cut and the diameter of black portion was measured at different locations and the average value was taken.

Oxidation index is determined by the formula:

$$\text{Oxidation index} = (\text{Area of oxidized zone} / \text{Total area}) \times 100$$

Lower oxidation index indicates the higher oxidation resistance of the brick.

It may be noted that conventionally the oxidation resistance tests are carried out by firing the samples at 1400 °C for 5 hours. However we have used a much more stringent test standard for measuring oxidation resistance of our specimens.

4.4.8 Thermal shock resistance:

Thermal shock/thermal spalling is the direct result of exposing the refractory installations to rapid heating and cooling conditions which cause temperature gradients within the refractory. Such gradients cause an uneven thermal strain distribution through the sample, may cause failure of the material.^[83, 84] The standard method of finding out spalling resistance is heating the material at an elevated temperature followed by sudden cooling in air at ambient temperature. The thermal shock resistance of refractory materials is determined using standard quench tests^[85, 86] in which the material is heated and cooled subsequently and the number of heating & cooling cycles that a material can withstand prior to failure is taken as its thermal shock resistance. The quantification was done by the number of cycles to withstand such temperature fluctuations. The samples are heated at 1400 °C for 10 minutes and then suddenly brought down to ambient conditions by cooling it in the air for 10 minutes. The number of cycles before any cracks in the specimen was noted down as the thermal shock resistance.

4.4.9 Static slag corrosion test:

Slag corrosion test by static crucible method was done for all the different compositions at 1600 °C for 4 h with Blast Furnace slag. Chemical composition (%) and basicity of the Blast Furnace slag are given in table .The sections after slag attack are visually compared and corroded dimensions were taken.

Table.4.10: Chemical composition (wt. %) and basicity of the steel making Blast Furnace slag. ^[87]

Constituent	Mean Percent (%)
Calcium oxide (CaO)	34-43
Silicon oxide (SiO ₂)	27-38
Aluminum Oxide (Al ₂ O ₃)	7-12
Magnesium oxide (Mgo)	7-15
Iron (FeO or Fe ₂ O ₃)	0.2-1.6
Manganese oxide (MnO)	0.15-0.76
Sulfur(S)	1-1.9

4.4.10 Permanent Linear change (PLC) on reheating:

In materials certain permanent changes occur during heating and these changes occur due to; change in the allotropic form, chemical reaction, liquid phase formation, sintering reactions

$$\text{PLC (\% linear)} = (\text{Increase or decrease in length/ original length}) \times 100$$

With the help of these changes determined the volume stability, expansion and shrinkage of the refractory at high temperatures.

Chapter – 5

Results & Discussion-I Effect of STG amount on ASC Refractories

5.1 Structure and chemistry of graphite and special treated graphite:

With the help of XRD and FESEM natural graphite was investigated. Natural graphite was characterized from the points of view of their particle size, crystallinity, purity etc.

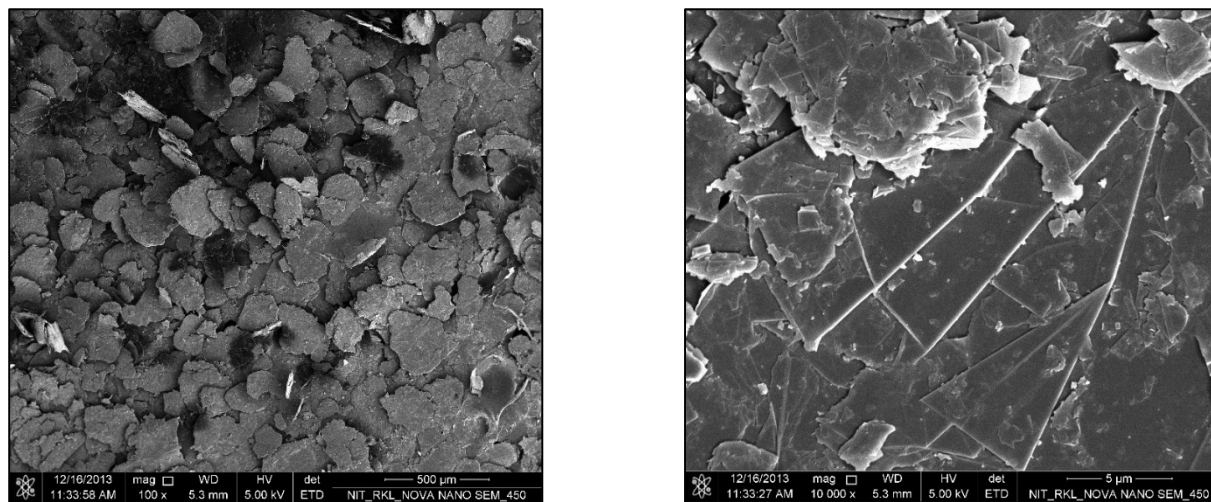


Fig.5.1: SEM images of natural graphite. The left image indicates the lateral size of the graphite flakes and the right image is a magnified image of the surface of a flake.

From FESEM images (Fig.5.1) it was observed that natural graphite is flaky in nature. It can be observed from the electron micrograph that the lateral dimension of graphite flakes is more than 200 μm .

XRD graph of natural graphite are presented in Fig.5.2. The peaks at 26.56° and 54.69° are consistent with the (002) and (004) peaks of graphite respectively. The small bump at 24° can be explained with trace amount of SiO_2 that is present in natural graphite. (Note that the fixed carbon content in the used graphite is only 94%, which is considerably on the lower side.)

Thermal analysis was done in argon atmosphere up to a temperature of 700°C at a heating rate of 10°C/min. Results of TGA analysis of natural flake graphite samples are presented in Fig.5.3. The graph shows mass loss of <1.5% up to 300°C. This weight loss occurs due to the moisture in graphite. After that weight loss is negligible.

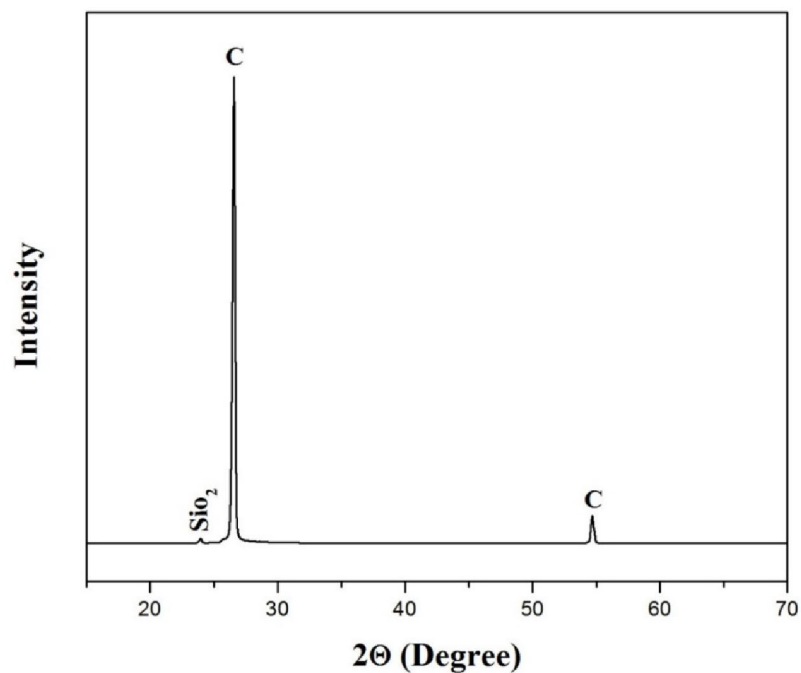


Fig.5.2: X-ray diffraction of graphite

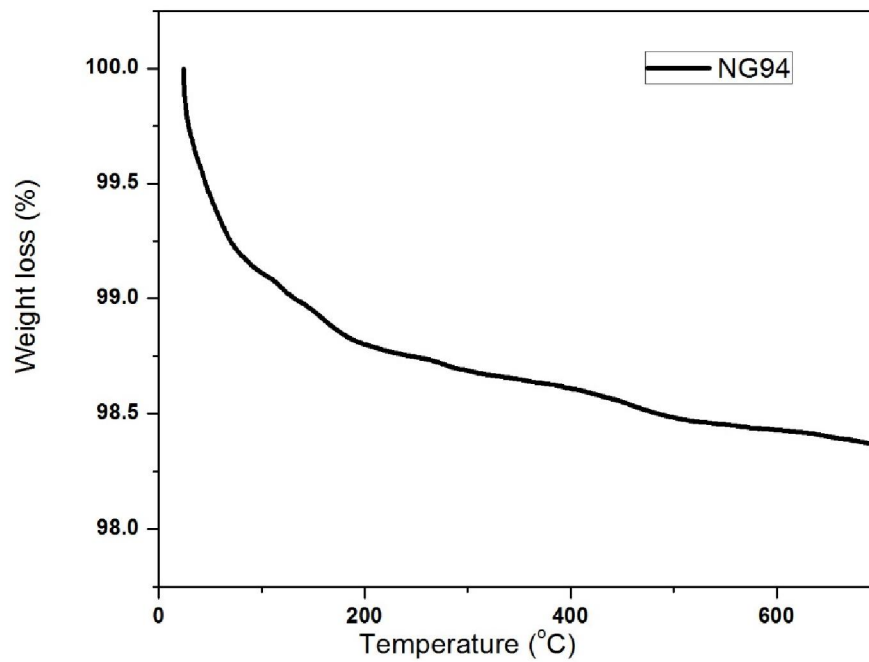


Fig. 5.3: Thermal analysis of the natural flake graphite (94FC) sample

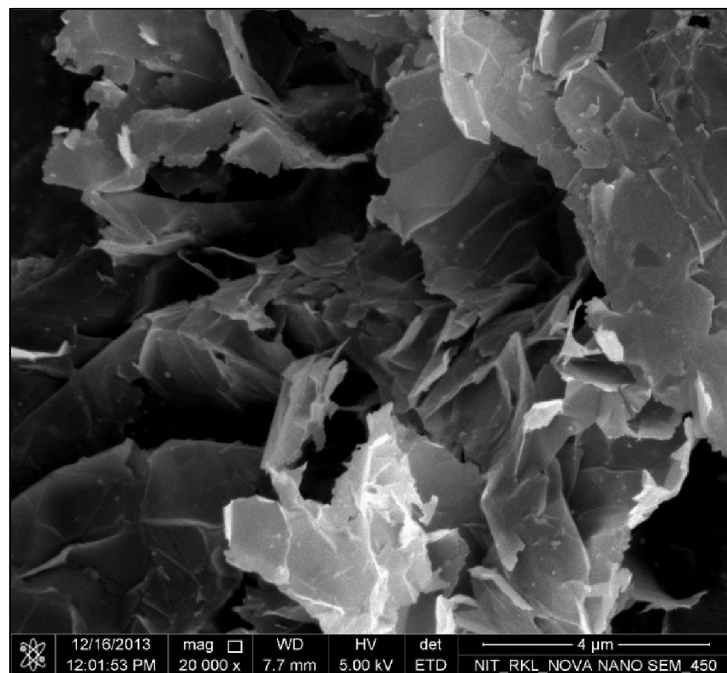


Fig. 5.4: FESEM images of STG

On the other hand, the specially treated graphite was quite voluminous as compared to natural graphite. From the FESEM images of STG (Fig. 5.4) it was clear that the natural graphite was expanded. After treatment the graphite flakes were expanded perpendicular to the graphene layers. Spacing between the graphene layers increased up to 30 μm and exposed.

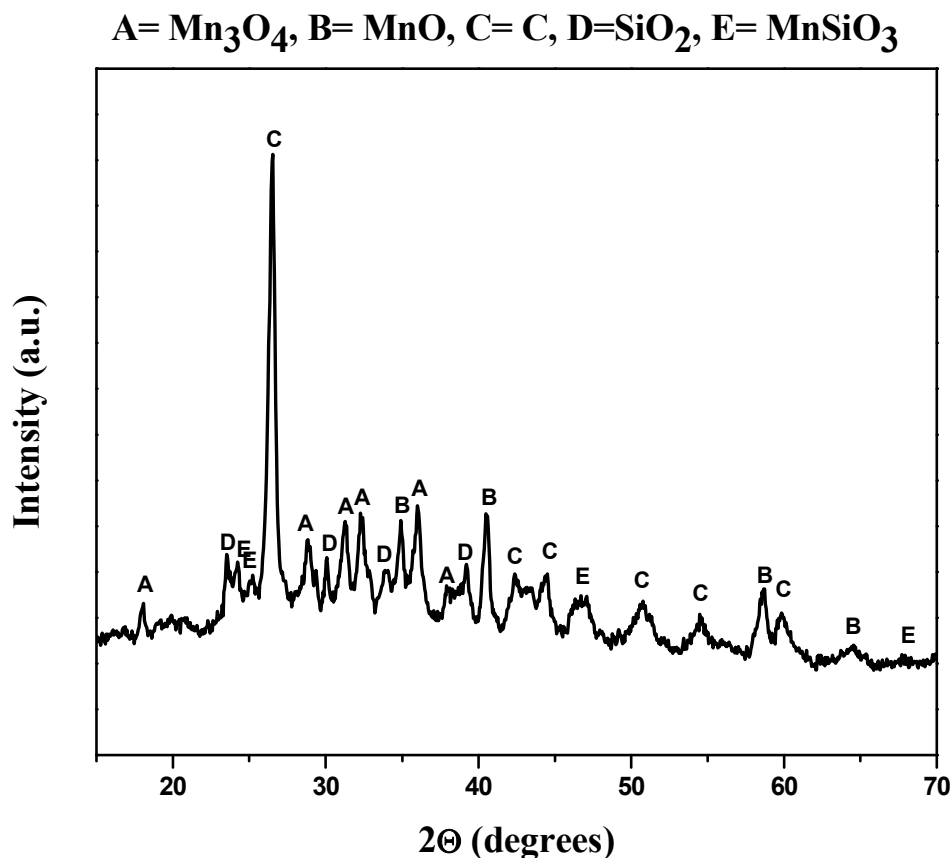


Fig.5.5: X-ray diffraction pattern of STG

XRD pattern of exfoliated graphite is similar to the natural graphite except some extra impurity peaks which came due to the presence of manganese oxide. There is a lot of difference in the peak intensities. Natural graphite shows a great, sharp and regular peak shape because of its high crystallinity. STG shows a peak with reduced intensity.

This means that after intercalation, the thick layered graphite crystals have broken down to tiny graphitic domains with reduced layer size. The interplanar spacing between graphene layers has not changed, which is evident from the fact that the (002) peak remains at the same 2 theta angle. We see that the peak has changed from 6133340 counts to about 5750.82 count.

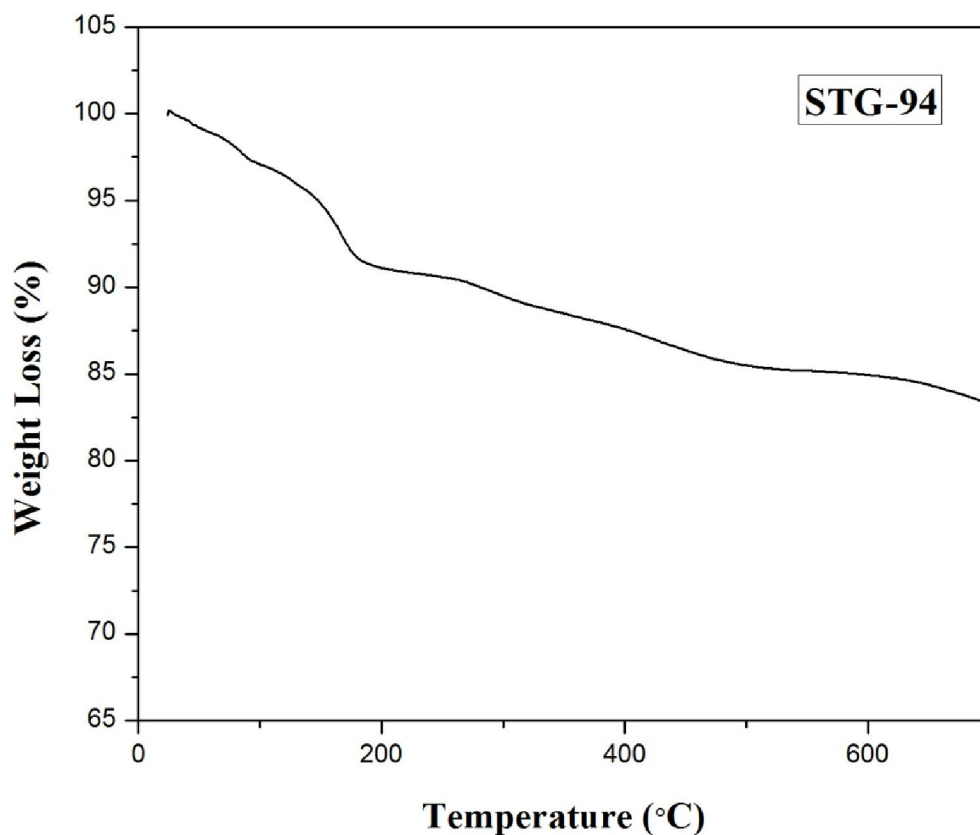


Fig.5.6: Thermal analysis of the STG

Thermogravimetric analysis of STG indicates that its behavior is slightly different than that of natural graphite. The mass loss over 700-800°C was about 15% and it remained steady after 20% loss. The loss is due to the removal of volatiles, such as nitrates (from nitric acid), potassium etc. It was found from carbon analysis that the carbon content in STG is ~ 80%.

5.2 Effect of STG amount on ASC Refractories:

In this section, evaluation of the various thermo mechanical properties of ASC refractory is presented with the emphasis on the effect of the amount of STG in the refractory composition.

5.2.1 Physical properties before coking:

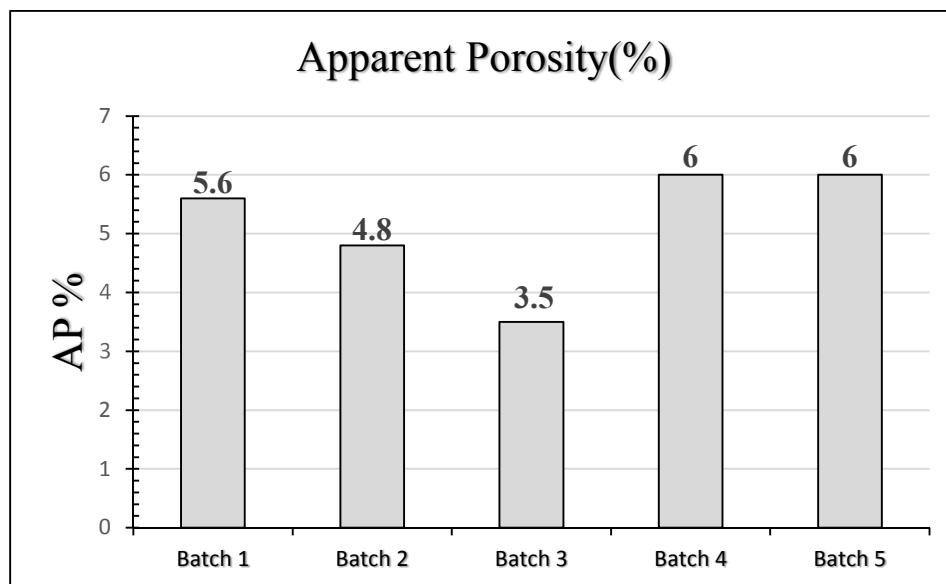


Fig.5.7: Variation of apparent porosity with the variation of STG content

The change in AP with the increase of STG is shown in Fig.5.7. AP has the value of 5.6 without any STG and has the value 3.5 for 1.5 wt% STG. This decrease in AP is because of addition of STG increases the filling of spaces between bigger refractory particles. Thus overall the porosity decreases. But in case of 1.75 to 2 wt% STG AP increases again. The exact reason for the increase in AP for 1.75 and 2% STG could not be ascertained.

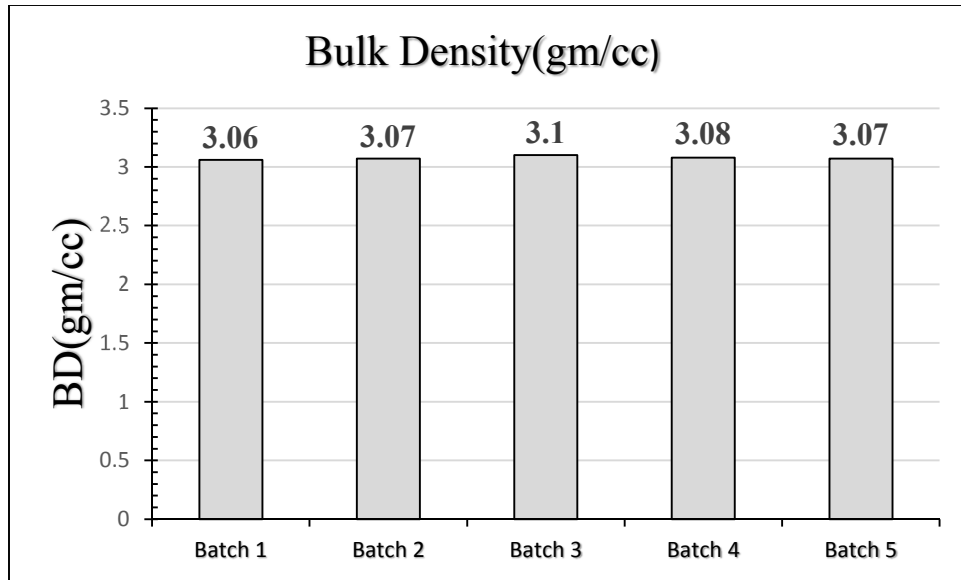


Fig.5.8: Variation of bulk density with the variation of STG content

The variation of bulk density is shown in Fig.5.8. The variation of bulk density with the STG is very less which ranges from 3.06 gm/cc to 3.1 gm/cc. The bulk density without the STG was 3.06 gm/cc. With the increase of STG content better pore filling is done which due to it higher bulk density. However, despite being a very low specific gravity material, the 1.75 and 2 wt% STG (in place of similar amount of natural graphite) reach BD values similar to the unmodified sample (batch 1). This indicates better packing in the STG based samples in general. Of course, sample 3 indicates best bulk density of all of the batches considered.

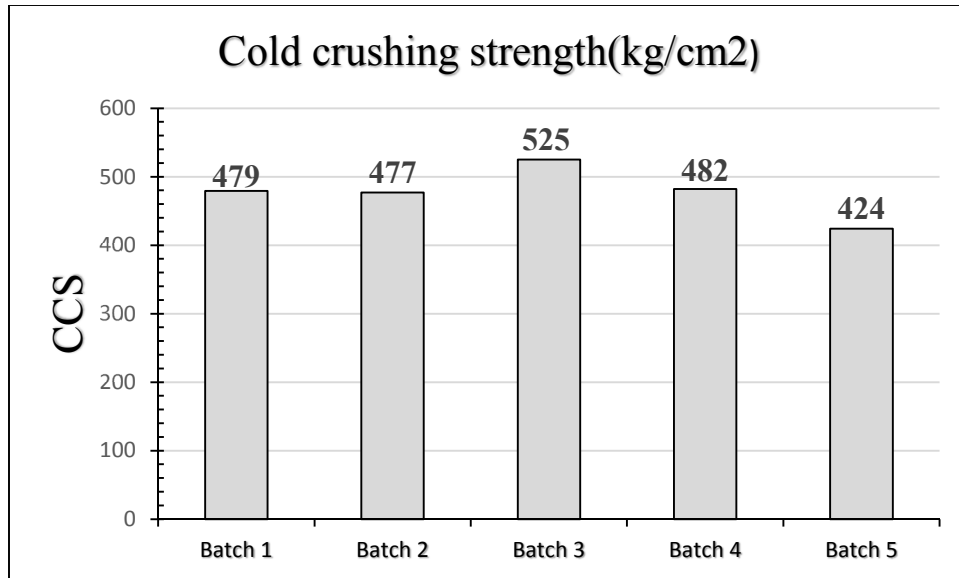


Fig.5.9: Variation of cold crushing strength with the variation of STG content

The variation of cold crushing strength with the STG is shown in Fig.5.9. From the figure it is clear that with the increase of STG cold crushing strength increases. The CCS value of the sample which contains no STG is 479 kg/cm² but for 1.5 wt% STG added sample CCS value is 525 kg/cm², which is almost 10% higher as compared to batch 1. Increase in CCS may be assigned to better filling of pores and a higher BD. The trend of CCS for STG at other addition levels followed trends similar to that of AP and BD and values were roughly similar to CCS values for batch 1 (the sample without any STG).

5.2.2 Physical properties after coking:

Here, the AP, BD and CCS results for the samples they were coked at 1000°C are discussed.

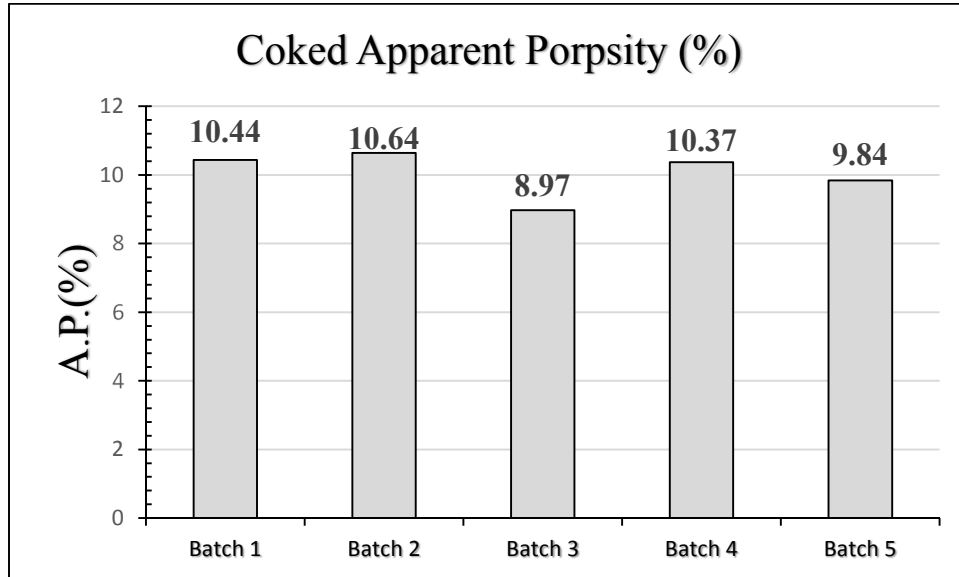


Fig.5.10: Variation in coked apparent porosity with the variation of STG content

The variation of apparent porosity of coked bricks is shown in fig.5.10. With the addition of STG the percentage of AP is reducing in similar fashion to AP of the samples before coking while 1.5 wt. % STG added samples gives the best value. AP values of coked samples increase because of the burning out of the organic species of the resin. Due to the burn out of the resin pores are created within the bricks which increase porosity. There is no change overall in AP for the standard as well as modified composition, except for batch 3 that show slight improvement.

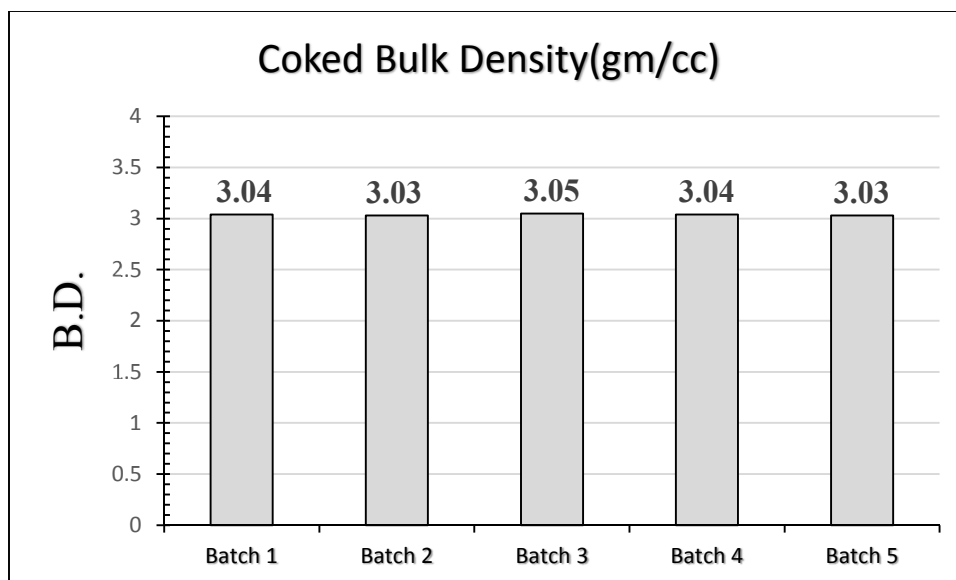


Fig.5.11: Variation of coked bulk density with the variation of STG content

The change in bulk density of coked samples is shown in fig.5.11. The values of bulk density vary from 3.03gm/cc to 3.05gm/cc, which is a very close range to distinguish. There is small variation in bulk density. The values decrease in comparison with bulk density of tampered samples. Similar to the previous tests here also the 1.5 wt. % STG added sample shows the best value which is 3.05gm/cc.

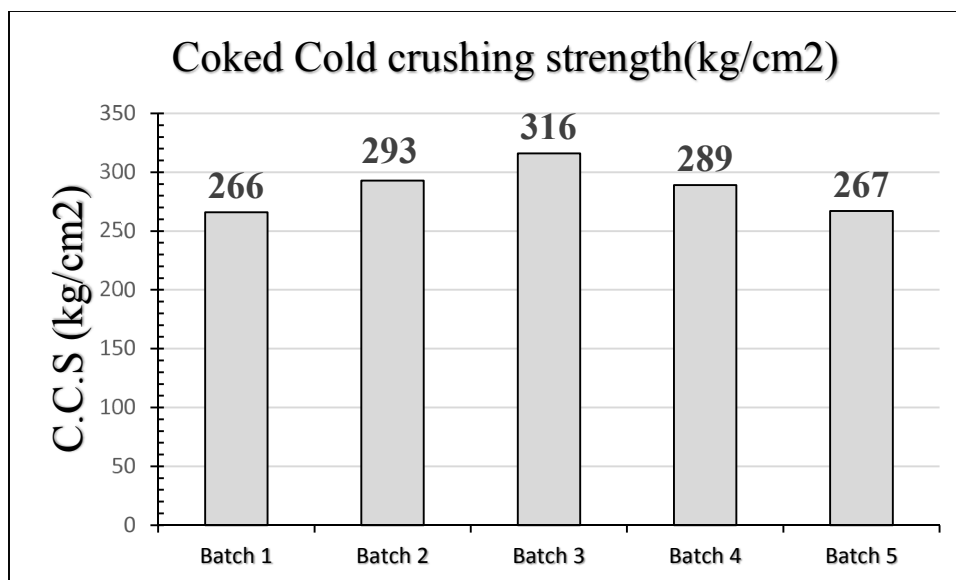


Fig.5.12: Variation of coked cold crushing strength with the variation of STG content

The coked CCS values are shown in fig.5.12. The CCS values of coked samples vary in between 266 kg/cm² to 316 kg/cm². From the figure it can be shown that the CCS values of coked samples change in similar fashion with tempered samples where 1.5 wt. % STG contained sample gives the best value. The CCS values of coked samples are lowered because of the breaking of the interlocking structure which has been created after polymerization of resole resin. The breaking of the interlocking texture occurs due to the burn out of the organic portion of the resin. In general, all of the STG added batches showed improved crushing strength which indicates that the distribution of various components of the refractory is homogeneous. In addition, batch 3 composition exhibited almost 19% increase in crushing strength as compared to the standard. This increment in value was better than its increment for CCS before coking.

5.2.3 Hot modulus of rupture:

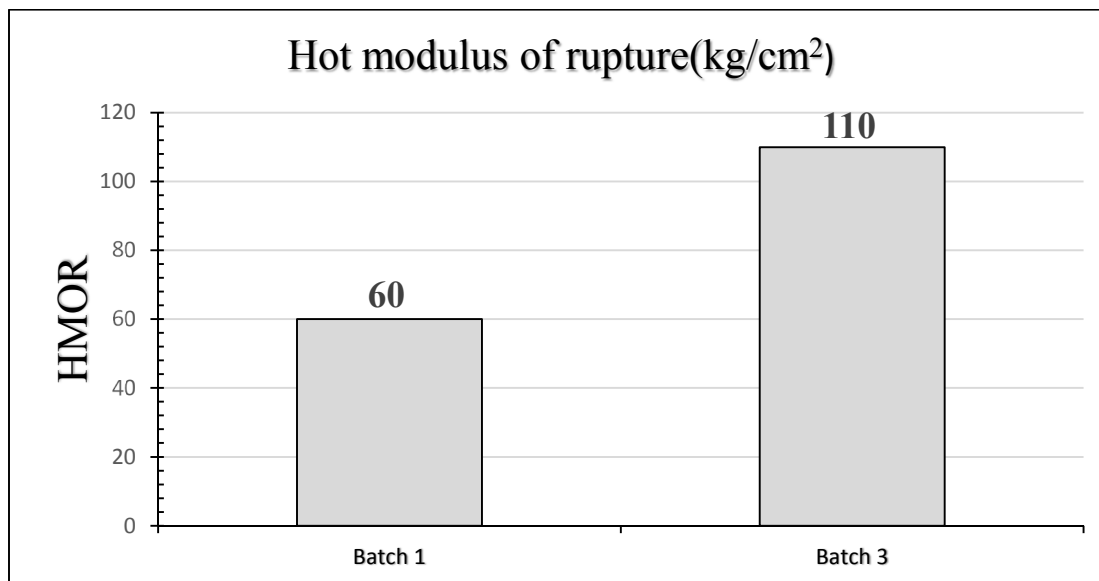
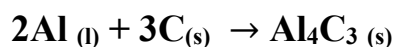


Fig.5.13: Variation of hot modulus of rupture with the variation of STG content

Based as the previous observation from physical properties, the hot strength values were compared between the standard sample (without STG) and the better performing sample (STG at 1.5%). Fig.5.13 shows the variation of HMOR values with 0 wt. % STG and 1.5 wt. % STG. There is a substantial improvement of HMOR for batch 3 at (1.5 wt. % STG) 110 kg/cm² in comparison to the without STG, which was 60 kg/cm². This is an increment of 83% in hot strength, which is exceptional for these types of bricks. With the STG pores inside the bricks fill better. So, the strength of the bricks enhances. Because of high surface area, STG is more reactive than graphite. So, at the high temperature, higher amount of carbide (Al₄C₃) forms by reacting with antioxidants.



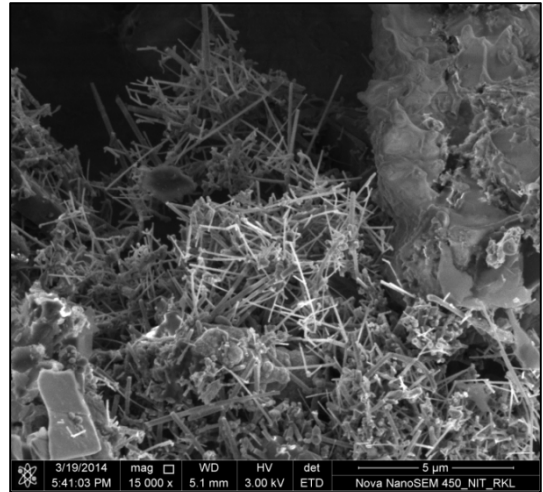
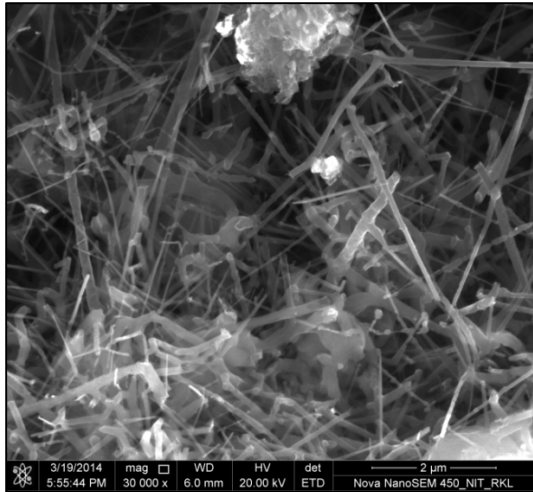


Fig. 5.14: FESEM images of 1.5 wt% STG at 1400°C

Fig.5.14 shows that, there is lots of fibers are present in 1.5 wt. % STG sample. According to this figure, we can see the fibers like structure and aluminum carbide whiskers and also aluminum nitride are present in the sample, which are responsible for higher strength and higher HMOR value of 1.5 wt. % STG.

5.2.4 Thermal shock resistance:

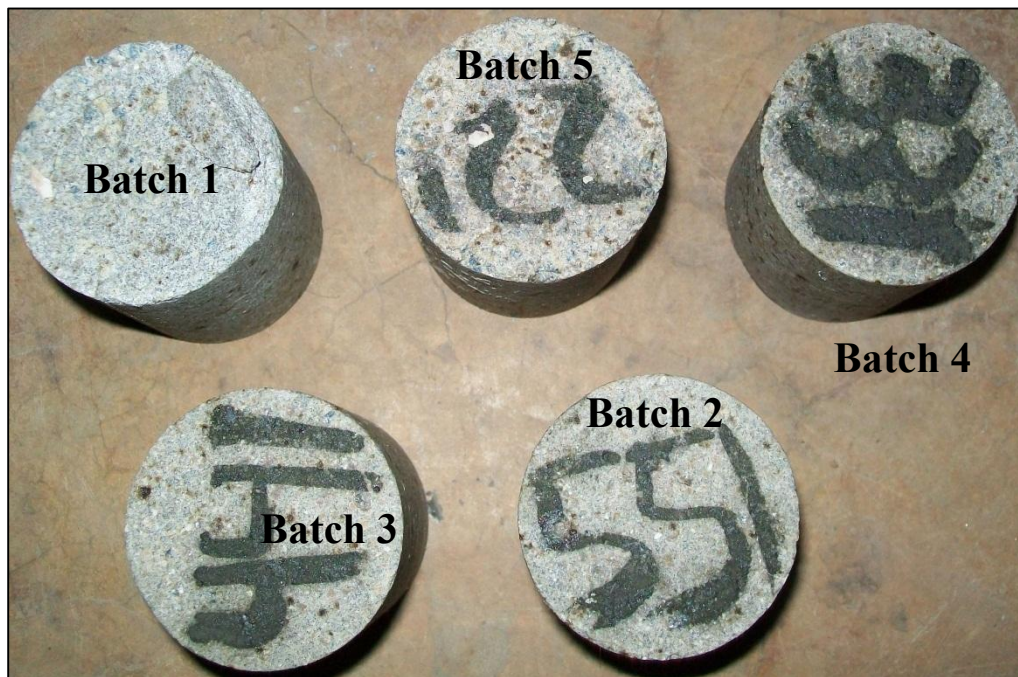


Fig.5.15: Samples after 12th cycle



Fig.5.16: Samples after 13th cycle



Fig.5.17: Samples after 14th cycle



Fig.5.18: Samples after 15th cycle



Fig.5.19: Sample after 16th cycle

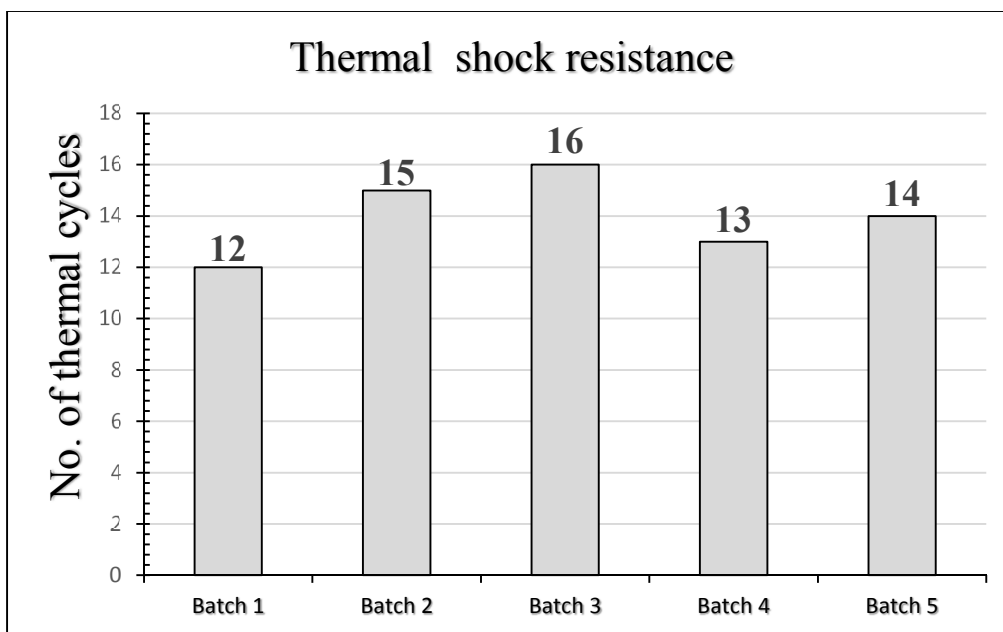


Fig.5.20: Graph of thermal shock resistance

The thermal shock resistance of different samples is shown in the above figures. Batch 3 which contains 1.5 wt. % STG shows a good result than batch 2 and 5. Batch 1 and batch 4 shatter after 12th and 13th thermal cycle, whereas the batch 5 and batch 2 sample shatter after 14th and 15th thermal cycle. Batch 3 gives the best result which stands without shattering even after 16th thermal cycle, with only a crack on its upper surface. Such improved thermal shock resistance than others because of the distribution of carbon into the entire matrix. Uniform formation of the new carbide ceramic phases from interlocking structure in the sub grain regions thus effectively prevents crack during thermal cycling.

5.2.5 Oxidation resistance:



Fig.5.21: Images of the cross-section of the ASC specimens with 0%, 1%, 1.5%, 1.75% and 2 % addition of the STG and oxidized at 1400°C for 10 hours

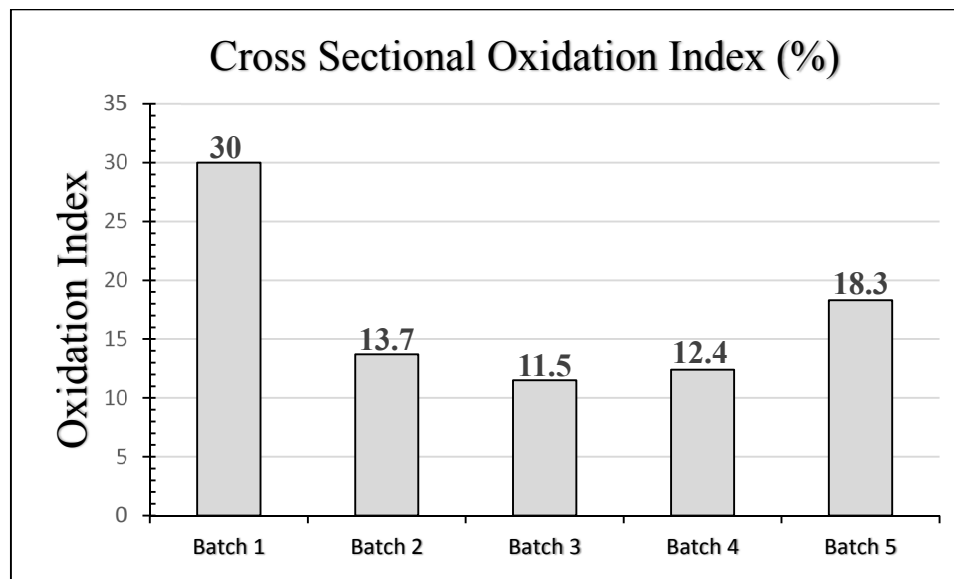


Fig. 5.22: Oxidation Index (%) of tempered ASC samples with 0%, 1%, 1.5%, 1.75% and 2% addition of the STG and oxidized at 1400°C for 10 hours

The variation of the oxidation index of the ASC samples with the addition of the STG is presented in Fig.5.21. You can see that the outside ring area around the cross section of sample batch 1 clearly shows whiter contrast. The amount of whiteness indicates the extent of oxidation. Almost 8-9 mm of the outside to inside is completely oxidized for sample of batch 1. This

corresponds to an aerial oxidation of 30%. Even by looking at the other samples it is clear that the all of the STG modified samples exhibit better oxidation resistance.

According to Fig.5.22, there is a clear indication that the oxidation resistance of the samples increases significantly with the addition of the STG. The oxidation index values decrease with STG from 30% to 11.5%. As STG forms carbide phases which have higher oxidation resistance property than that of natural graphite so, the oxidation index decreases with the STG for a certain amount of STG after a fix amount if we increased STG then again oxidation index increased. According to fig. 5.23 and 5.24 it is clear that, 1.5 wt. % STG having batch made more fibers like structures and aluminum carbide whiskers, aluminum nitride and silicon carbide in comparison to with 0 wt. % having samples, so STG is responsible for higher oxidation index.

FESEM images of 0 wt% or without STG after oxidation inner part (no oxidized part):

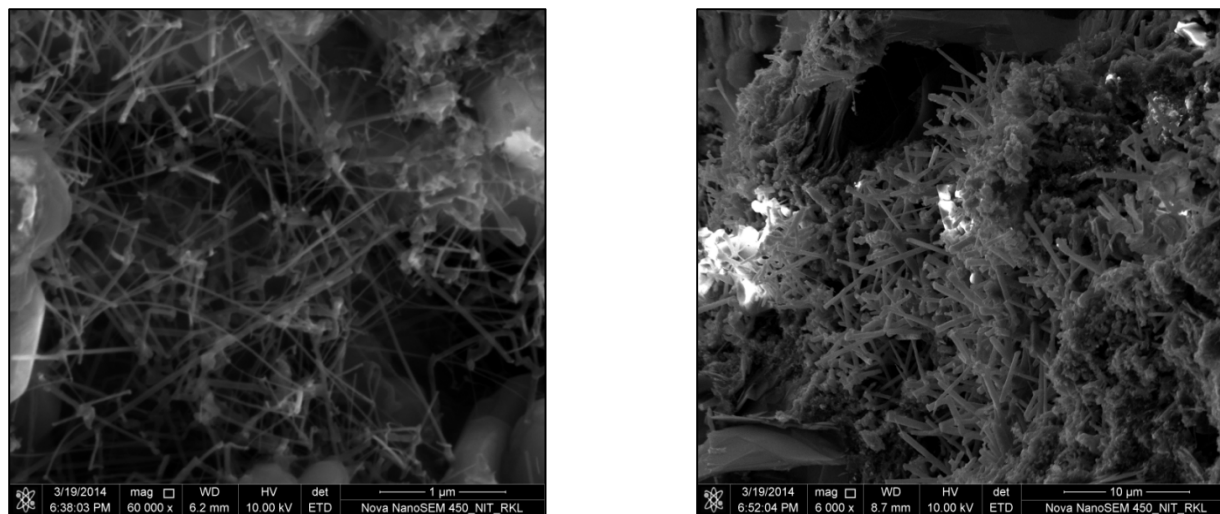


Fig. 5.23: FESEM images of 0 wt% STG after oxidation

FESEM images of 1.5 wt% STG after oxidation inner part (no oxidized part):

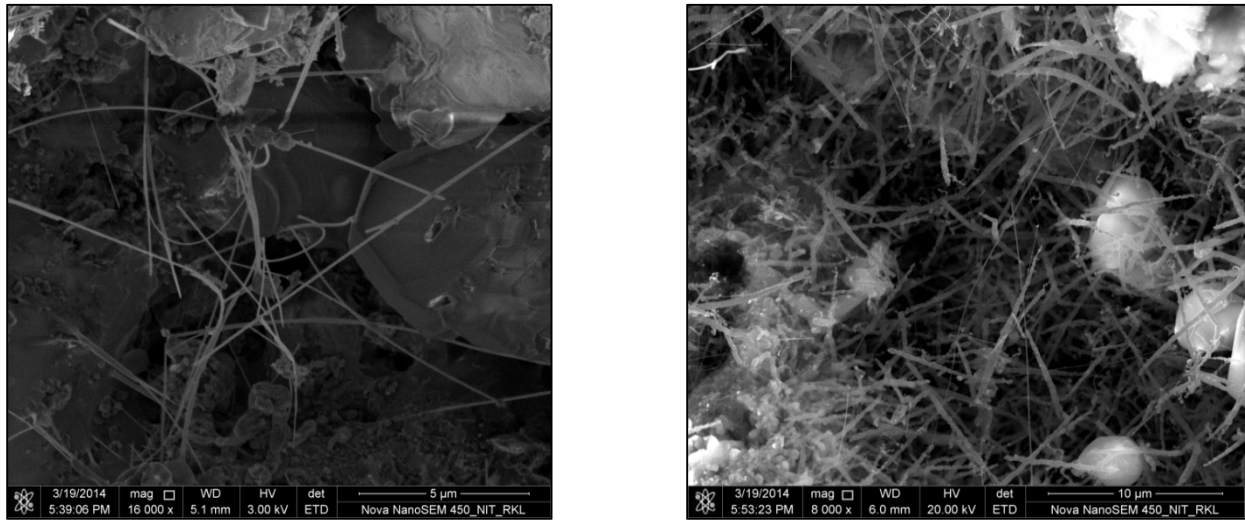


Fig. 5.24: FESEM images of 1.5 wt% STG after oxidation

5.2.6 Corrosion resistance:



Fig.5.25: Corroded samples before cutting with 0%, 1%, 1.5%, 1.75% and 2 % addition of the STG



Fig.5.26: Corroded samples after cutting with 0%, 1%, 1.5%, 1.75% and 2 % addition of the
STG

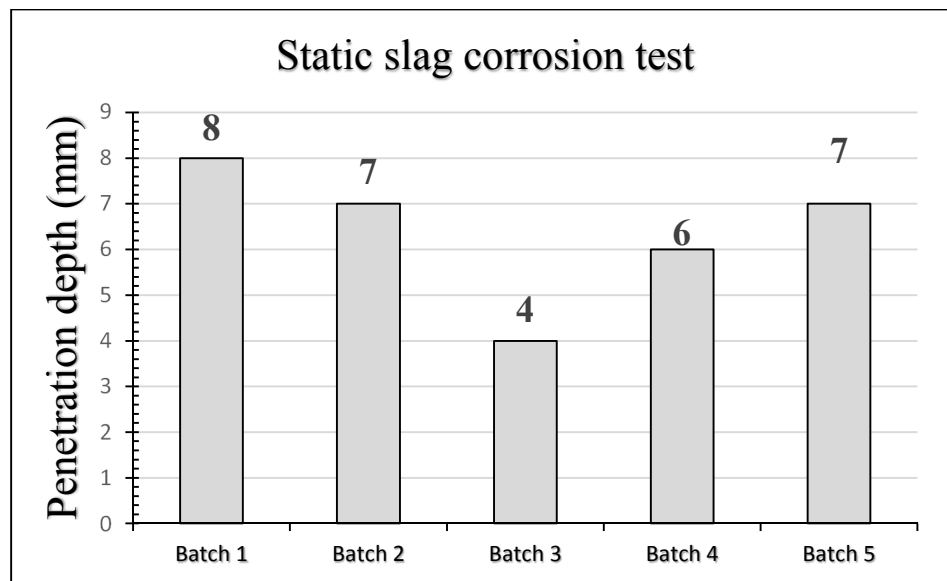


Fig.5.27: Graph of penetration depth of Static slag corrosion test

Fig.5.27 shows corrosion (mm) as a function of different amount STG and without STG added ASC refractories. It is clearly indicated that the 1.5 wt. % STG added samples undergone lowest corrosion. The penetration depth is lowering with the different STG percentage. But it is clear after 1.5 wt. % again penetration depth is increased. Due to STG, the distribution of carbon throughout the matrix is better and high in comparison to the without STG sample. Thus, corrosion resistance is high for STG containing samples.

5.2.7 Permanent Linear Change (PLC):

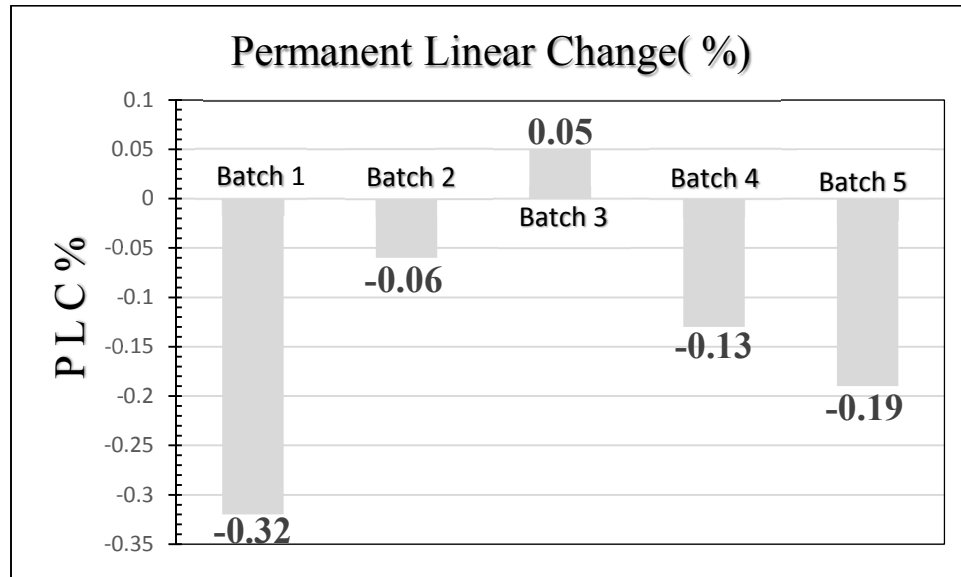


Fig.5.28: Graph of Permanent Linear Change (PLC %) test

Fig.5.28 shows PLC % as a function of different amount STG and without STG added ASC refractories. PLC value is positive (0.05) for 1.5 wt. % STG. For other composition PLC values are negative, but there is sharp difference between without STG and STG having samples. So it is clear that with the addition of STG the PLC values of ASC refractory is improved. Because with the STG addition ASC refractory shows phase transformation earliest at lowest temperature and liquid phase formation due to the more reactivity of the STG.

Chapter – 6

Results & Discussion-II **Effect of STG/Al₂O₃** **mixture ratio on ASC** **Refractories**

Effect of STG/Al₂O₃ mixture ratio on ASC refractory:

In this chapter the effect of STG/Al₂O₃ mixture ratio on various properties is explored. All of the experimental procedures was done as detailed in the previous section. With regards to change in composition investigated here, according to table 4.6. We have identified batch 3 as the best composition. Based on these composition a slight change in STG/Al₂O₃ mixture was performed. In batch 3 mixture ratio of alumina and STG was taken as 5:1 and in batch 6 alumina and STG ratio was 2:1.

6.1 Physical properties (before coking):

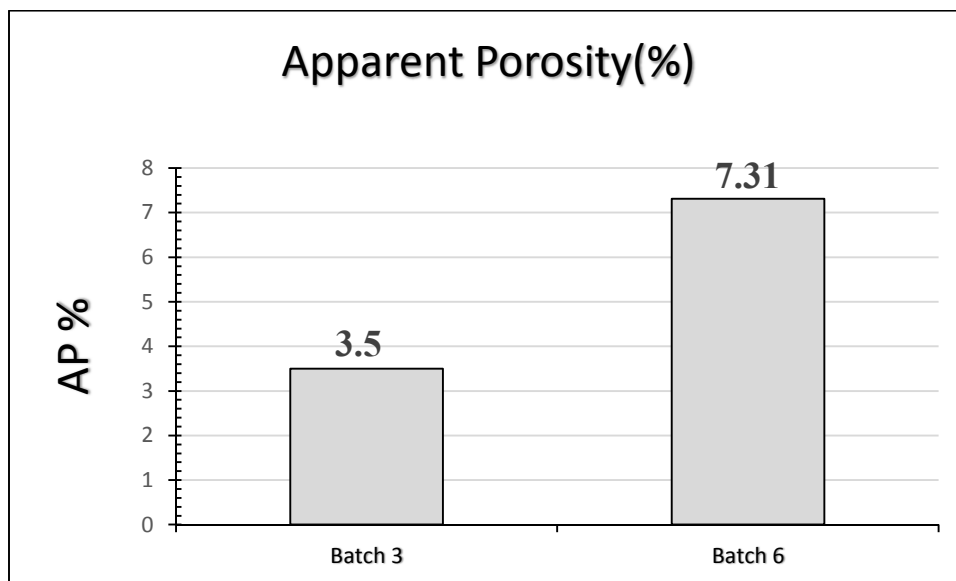


Fig.6.1: Variation of apparent porosity with the variation of STG/Al₂O₃ mixture ratio

The change in AP with the variation of STG/Al₂O₃ mixture ratio is shown in fig.6.1. With the change of mixture ratio of STG/Al₂O₃ the percentage of AP is increasing. The AP value increases for batch 6. Since the ratio of STG to Al₂O₃ was low in the composition, evidently the

distribution of STG in the refractory compact is not homogeneous. There may be region where STG has a higher concentration, than other region. Thus may have caused the increase in AP. The variation of bulk density is shown in fig.6.2. The bulk density appeared not to change very much, it is difficult differentiate between 3.1 and 3.07.

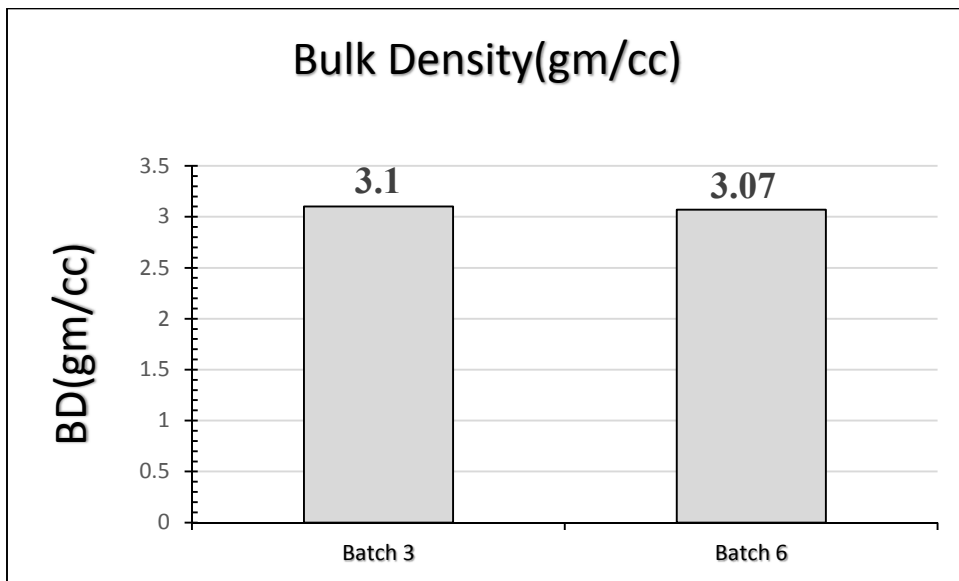


Fig.6.2: Variation of Bulk Density with the variation of STG/Al₂O₃ mixture ratio

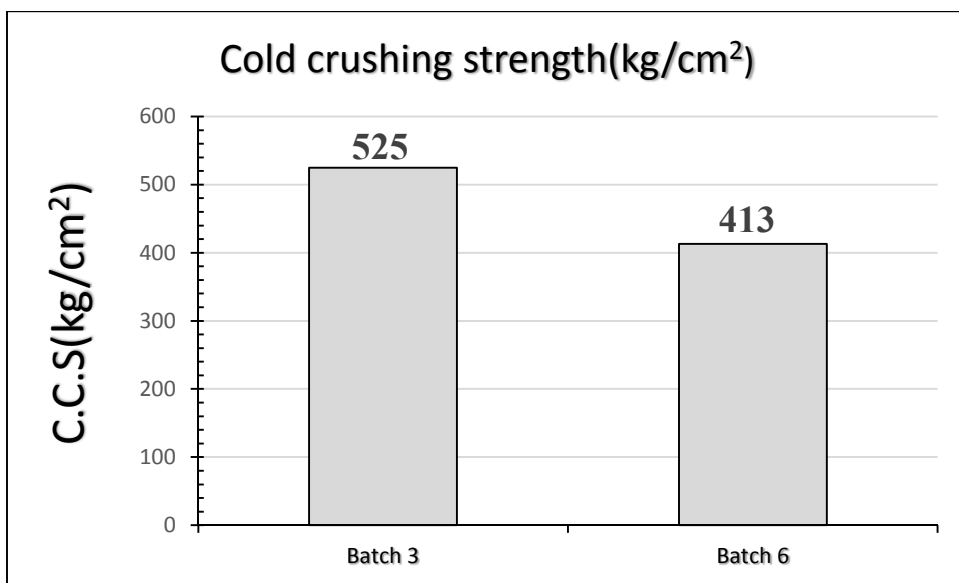


Fig.6.3: Variation of cold crushing strength with the variation of STG/Al₂O₃ mixture ratio

The variation of cold crushing strength is shown in fig. 6.3. The CCS value also decreases for batch 6. In the case of batch 6 there is improper filling of pores due to which CCS value is decreased. The distribution of the resin around the aggregates may also be the reason for decrease in strength.

6.2 Physical properties (after coking):

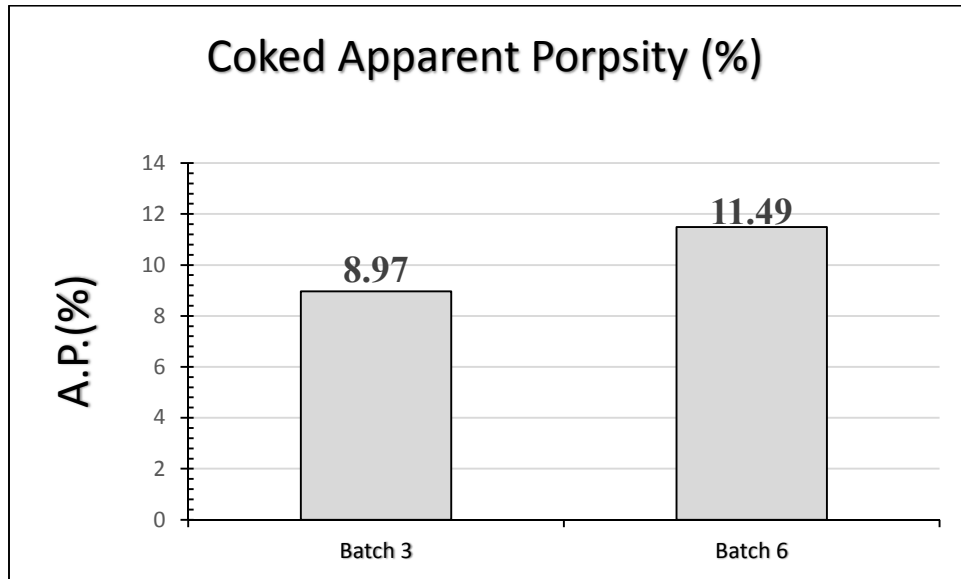


Fig.6.4: Variation of apparent porosity with the variation of STG/Al₂O₃ mixture ratio

The change in coked AP with the variation of STG/Al₂O₃ mixture ratio is shown in fig.6.4. With the change of mixture ratio of STG/Al₂O₃ the percentage of AP is increasing. Due to the low ratio of alumina fines in the mixture, a similar trend to the tempered AP is also seen here. The coked bulk density (Fig.6.5) also follows a similar trend in that the BD for batch 6 decreases slightly to 3.02 gm/cc.

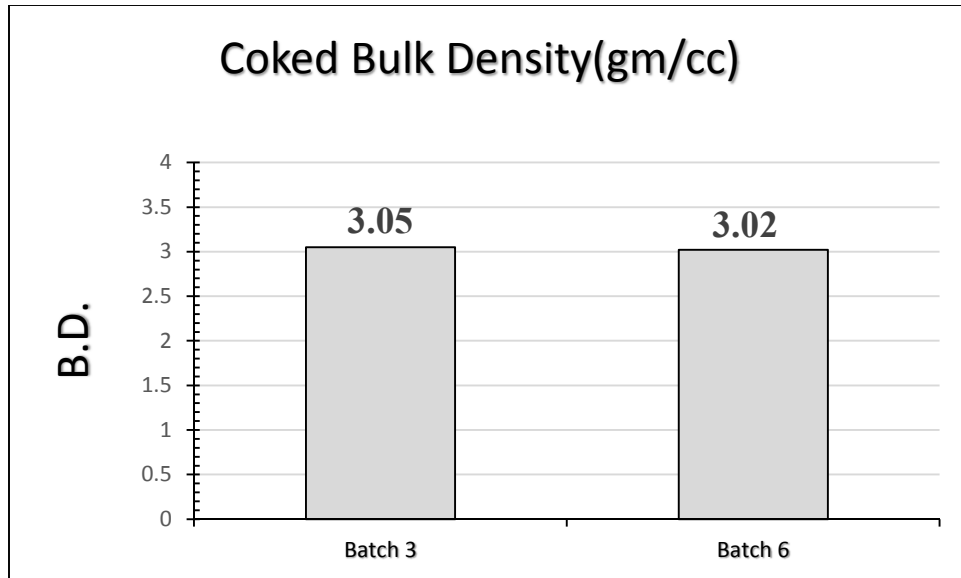


Fig.6.5: Variation of Coked Bulk Density with the variation of STG/ Al_2O_3 mixture ratio

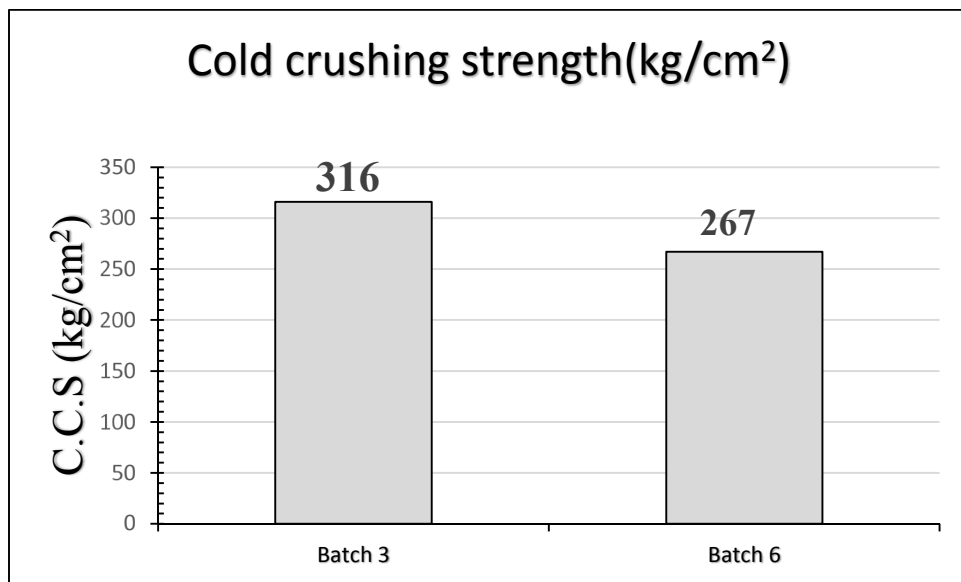


Fig.6.6: Variation of Coked cold crushing strength with the variation of STG/ Al_2O_3 mixture ratio

The variation of coked cold crushing strength is shown in fig. 6.6. The CCS value is also decreased of batch 6. In the case of batch 6 there is not proper filling of pores due to it CCS value is decreased.

6.3 Thermal shock resistance:



Fig.6.7: Samples after 13th cycle

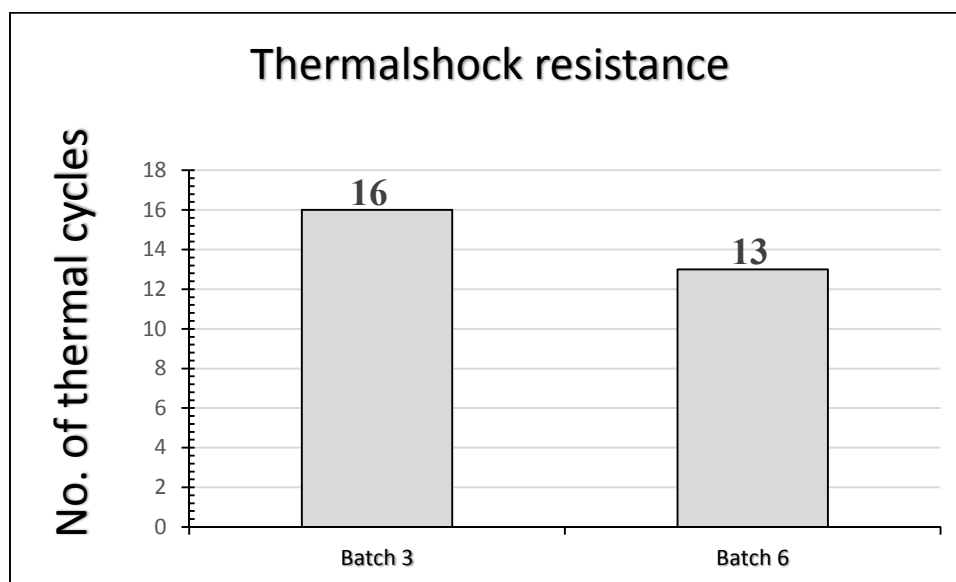


Fig.6.8: Graph of thermal shock resistance with the variation of STG/ Al_2O_3 mixture ratio

The thermal shock resistance of samples 3 and 6 are shown in the above figures. Batch 3 which contains 1:5 ratio of STG/ Al_2O_3 shows a good result than batch 6 which has 1:2 ratio of STG/ Al_2O_3 . In batch 6 value of thermal shock is decreased because in batch 6 fibers, aluminum nitrides and aluminum carbides formation are less in comparison to the batch 3.

6.4 Oxidation resistance:



Fig.6.9: Images of the cross-section of the ASC specimens of Batch 6 oxidized at 1400°C for 10 hours

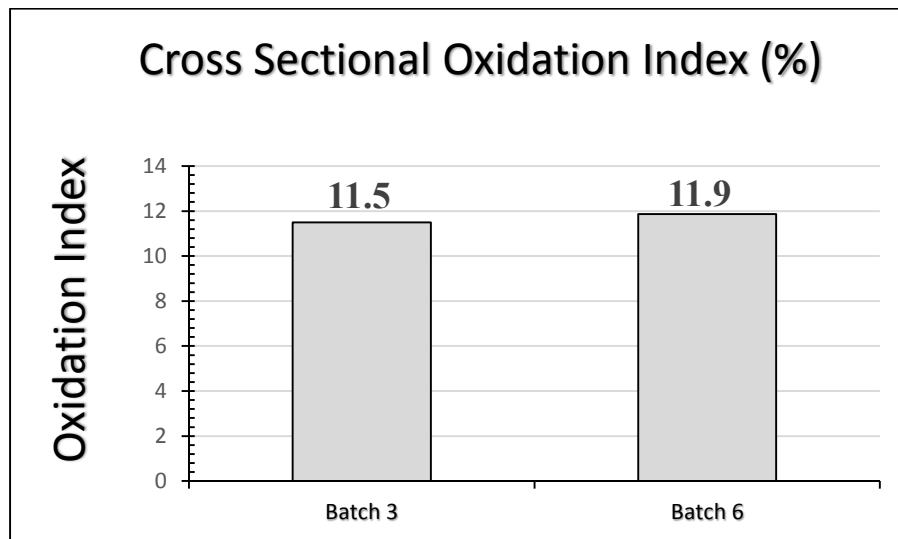


Fig.6.10: Oxidation Index (%) of tempered ASC Batch 3 and Batch 6 samples oxidized at 1400°C for 10 hours with the variation of STG/ Al_2O_3 mixture ratio

The variation of the oxidation index of the ASC samples with the variation of STG/ Al_2O_3 mixture ratio is presented in Fig.6.9 and 6.10. Oxidation image of batch 3 sample is given in Fig. 5.21. Interestingly, we have observed that there is practically no discernible difference in the

oxidation behavior of the batch 6 samples (Fig 6.9) as compared to there of batch 3 samples (Fig 5.21). Even after geometrically calculating the oxidation area as well as the oxidation index for the samples are 11.5 and 11.9%, for batch 3 and 6 respectively. These values are quit close to each other. It is unclear as to how the batch 6 sample exhibits good oxidation resistance, although the CCS has been found to be clearly interior to that of batch 3.

6.5 Corrosion resistance:



Fig.6.11: Corroded sample of Batch 6 after cutting

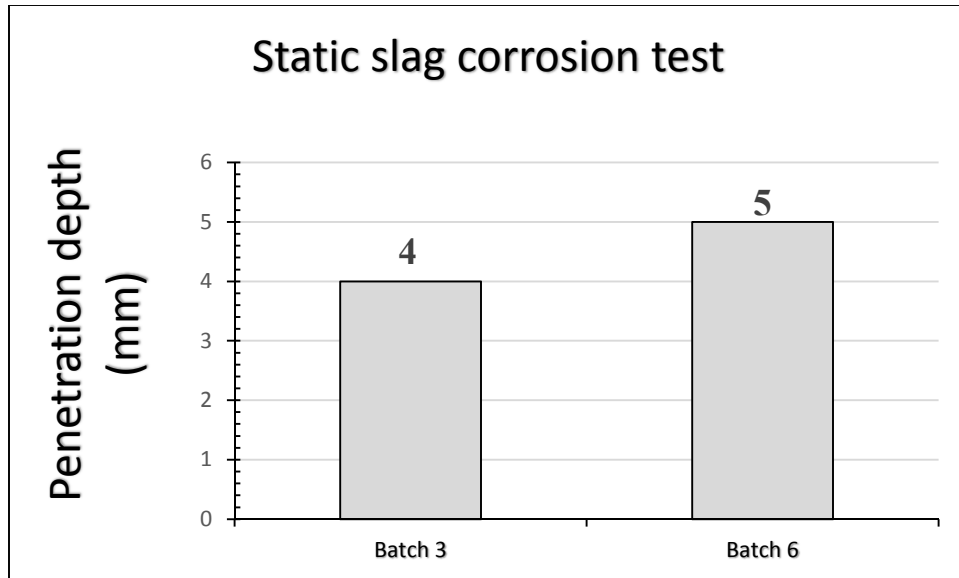


Fig.6.12: Graph of penetration depth of Static slag corrosion test with the variation of STG/ Al_2O_3 mixture ratio

Fig.6.12 shows corrosion (mm) as a function of the variation of STG/ Al_2O_3 mixture ratio ASC refractories. It is clearly indicated that the corrosion of batch 6 sample is more than the batch 3. The distribution of carbon throughout the matrix is not better in batch 6 due to the ratio of STG/ Al_2O_3 . Due to which the corrosion resistance is decreased.

Chapter – 7

Results & Discussion-III

Effect of the type of Alumina fines on ASC Refractories

In this chapter the effect of different alumina fines (calcined alumina and reactive alumina) on various properties is explored. All of the experimental procedures was done as detailed in the previous section. With regards to change in composition investigated here, according to table 4.7. In this section, we compare batch 7 with batch 6, in batch 7 reactive alumina is used, while in batch 6 calcined alumina used. Rest of the processes and composition etc. are kept the same.

7.1 Physical properties (before coking):

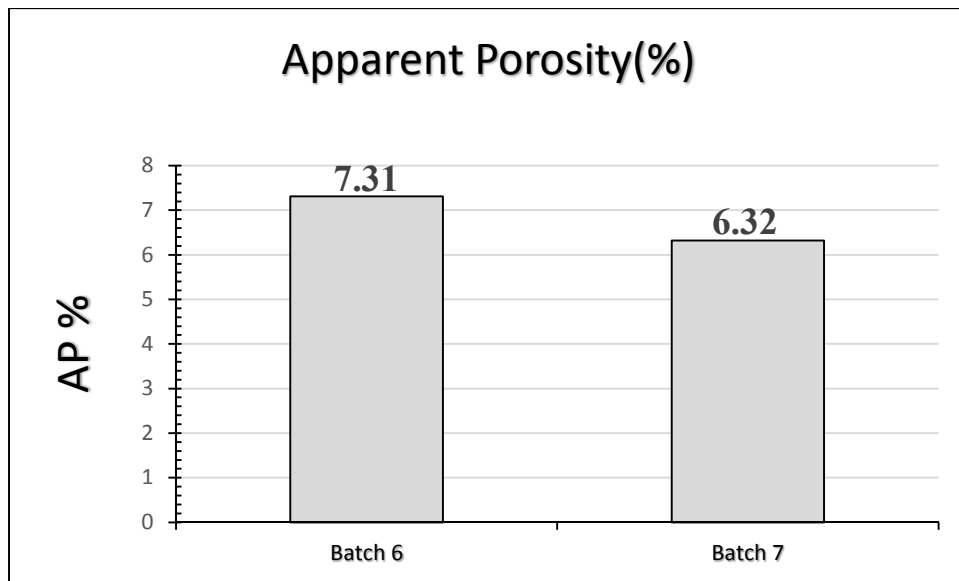


Fig.7.1: Variation of apparent porosity with the different –different alumina fines

The change in AP with the different alumina fines variation is shown in fig.7.1. The AP value is less for batch 7 as comparison to batch 6. In batch 7 reactive alumina used, which have small size as compared to the calcined alumina. The fineness of the alumina used can be expected to have increased the packing in the refractory composition, leading to (only slightly) lower apparent porosity. The variation of bulk density is shown in fig.7.2. There is slightly change in BD.

The variation of cold crushing strength is shown in Fig. 7.3. The CCS value decreases for batch 6. In the case of batch 6 there is calcined alumina size is slightly bigger not too much in comparison to reactive alumina due to which CCS value is slightly decreased as to batch 7. The distribution of the resin around the aggregates may also be the reason for decrease in strength.

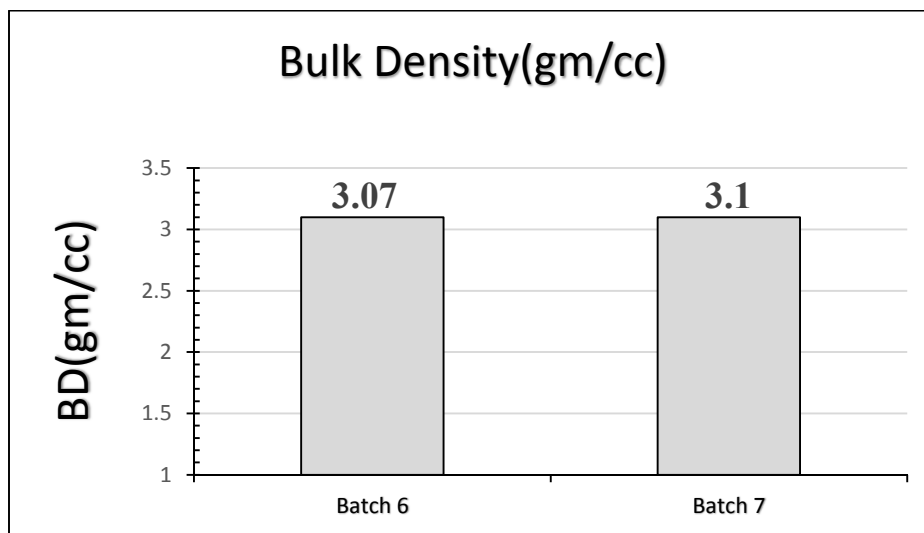


Fig.7.2: Variation of Bulk density with the different –different alumina fines

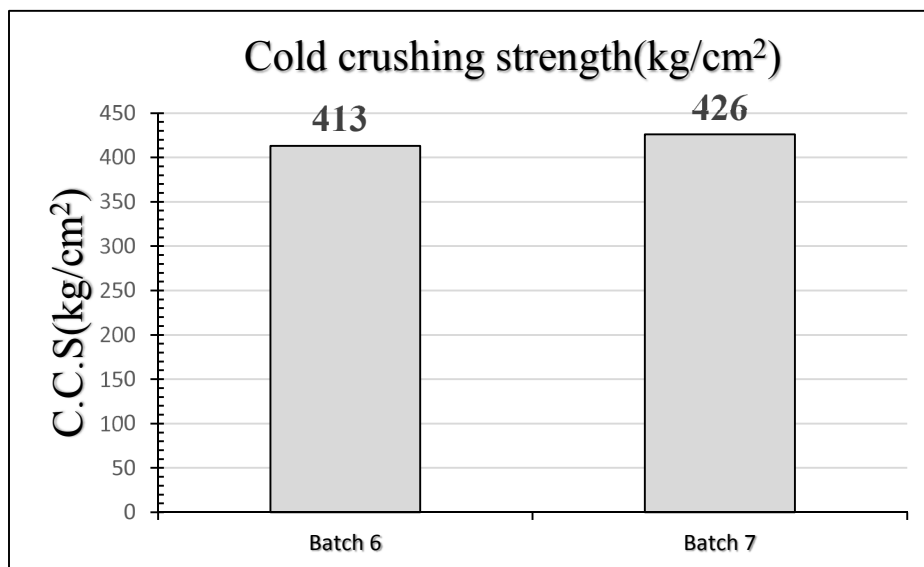


Fig.7.3: Variation of cold crushing strength with the different –different alumina fines

7.2 Physical properties (after coking):

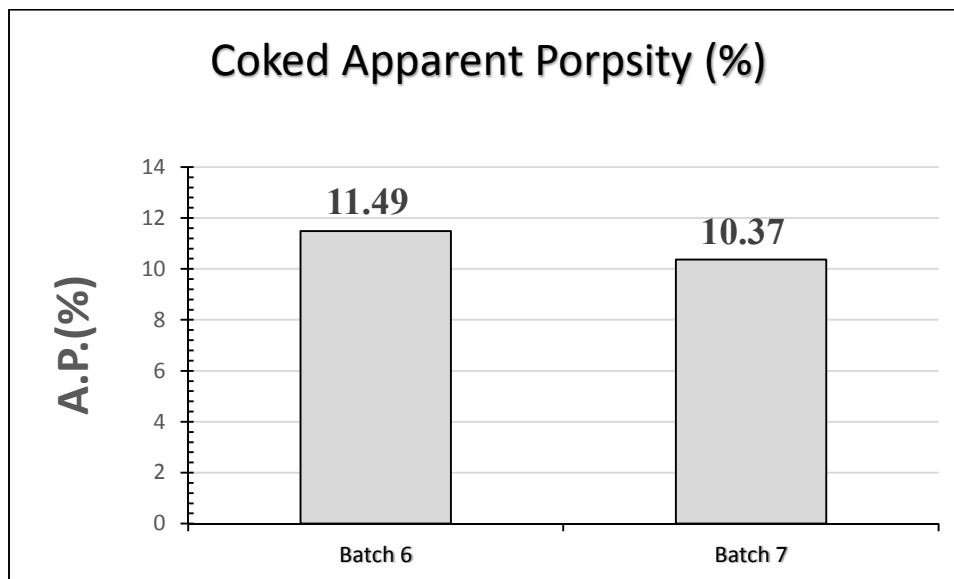


Fig.7.4: Variation of apparent porosity with the different –different alumina fines

The change in coked AP with the variation of different–different alumina fines is shown in fig.7.4. With the change of alumina fines the percentage of AP is decreasing for batch 7. Due to the size of alumina fines in the mixture, a similar trend to the tempered AP is also seen here. The coked bulk density (Fig.7.5) also follows a similar trend in that the BD for batch 6 decreases slightly to 3.02 gm/cc.

The variation of coked cold crushing strength is shown in fig. 7.6. The CCS value is also decreased of batch 6. The coked cold crushing strength appeared not to change very much, it is difficult to differentiate between 267 and 269.

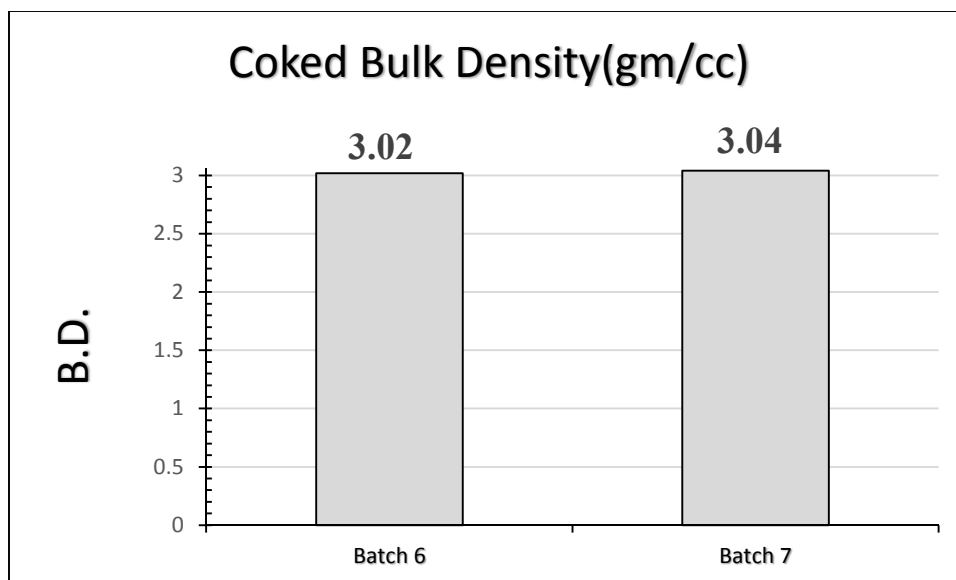


Fig.7.5: Variation of Bulk density with the different –different alumina fines

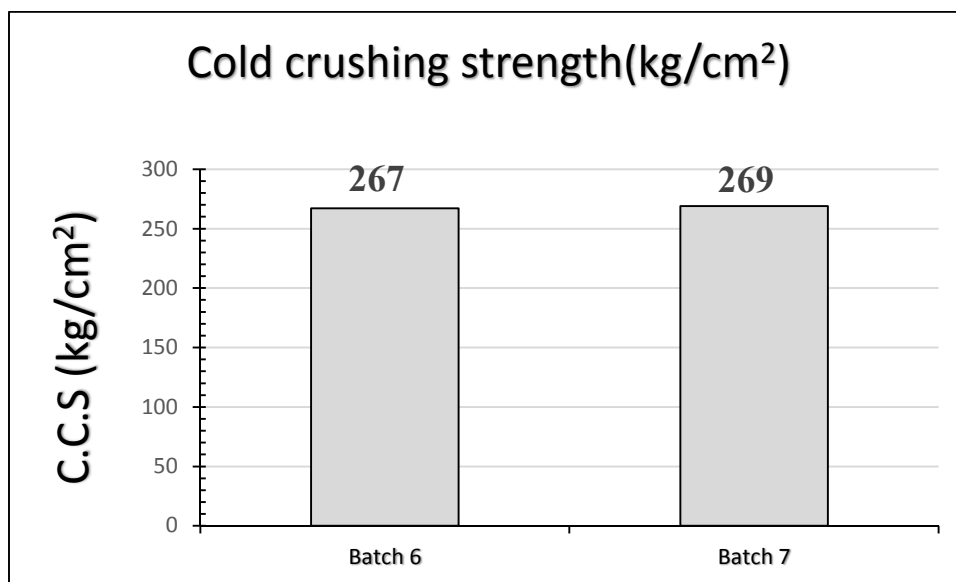


Fig.7.6: Variation of Coked cold crushing strength with the different –different alumina fines

7.3 Thermal shock resistance:

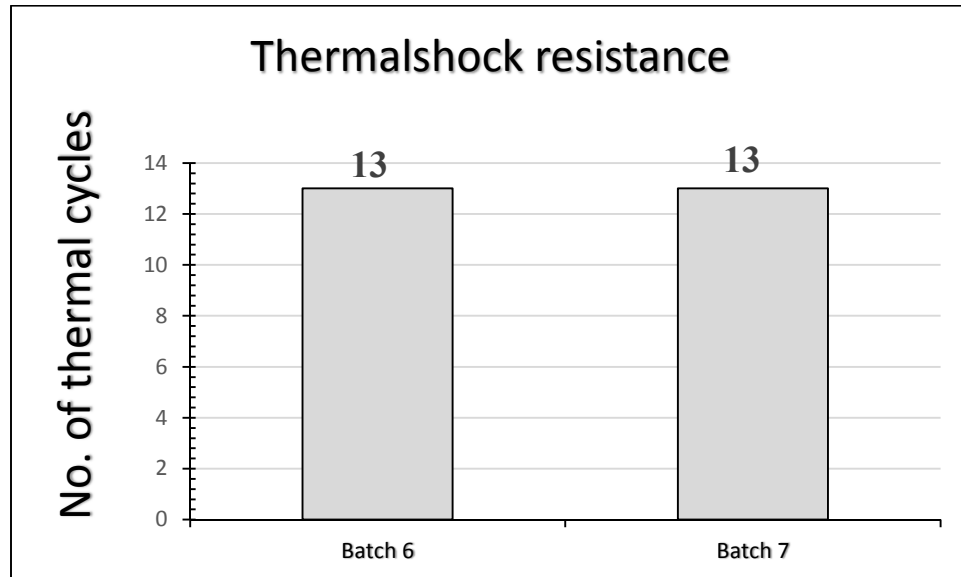


Fig.7.7: Graph of thermal shock resistance with the different –different alumina fines

The thermal shock resistance of samples 6 and 7 are shown in the fig. 7.7. The thermal shock resistance is similar for batch 6 and batch 7, because there is formation of aluminum carbides and nitrides are same. There is not too change in size of alumina fines of reactive alumina and calcined alumina, due to it most of properties are same for batch 6 and batch 7 remaining only AP.

7.4 Oxidation resistance:



Fig.7.8: Images of the cross-section of the ASC specimens of Batch 7 oxidized at 1400°C for 10 hours

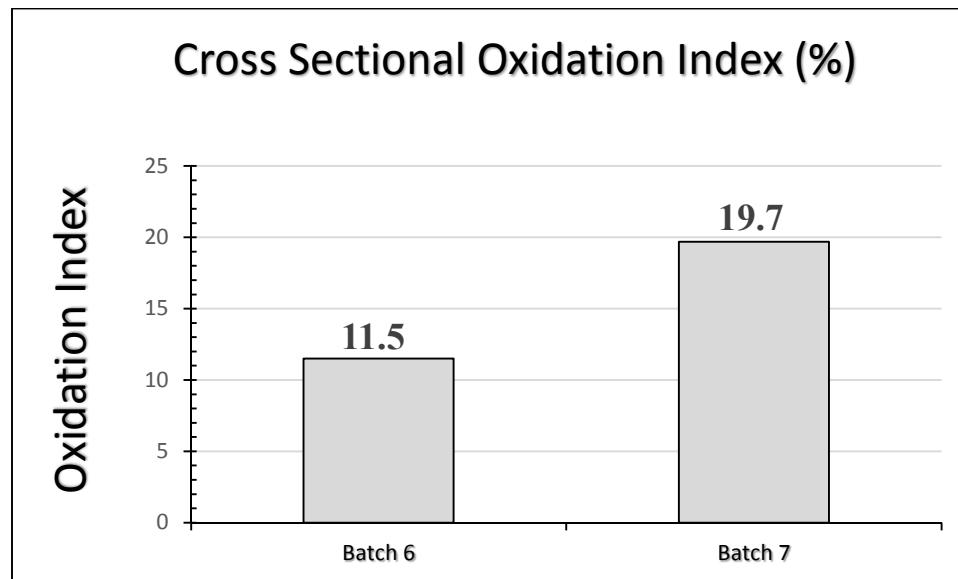


Fig. 7.9: Oxidation Index (%) of tempered ASC Batch 6 and Batch 7 samples oxidized at 1400°C for 10 hours with the different –different alumina fines

The variation of the oxidation index of the ASC samples with the variation of different–different alumina fines is presented in Fig.7.8 and 7.9. Oxidation image of batch 6 sample is given in Fig. 6.9. According to figures (6.9, 7.8 and 7.9) and geometrically calculating the oxidation area it is clear that oxidation is more in batch 7. Due to the small size of reactive alumina heat passing capacity is more in comparison to calcined alumina. Because of it more heat propagation occurs in batch 7 sample and as a result more oxidation occurs.

7.5 Corrosion resistance:



Fig.7.10: Corroded sample of Batch 7 after cutting

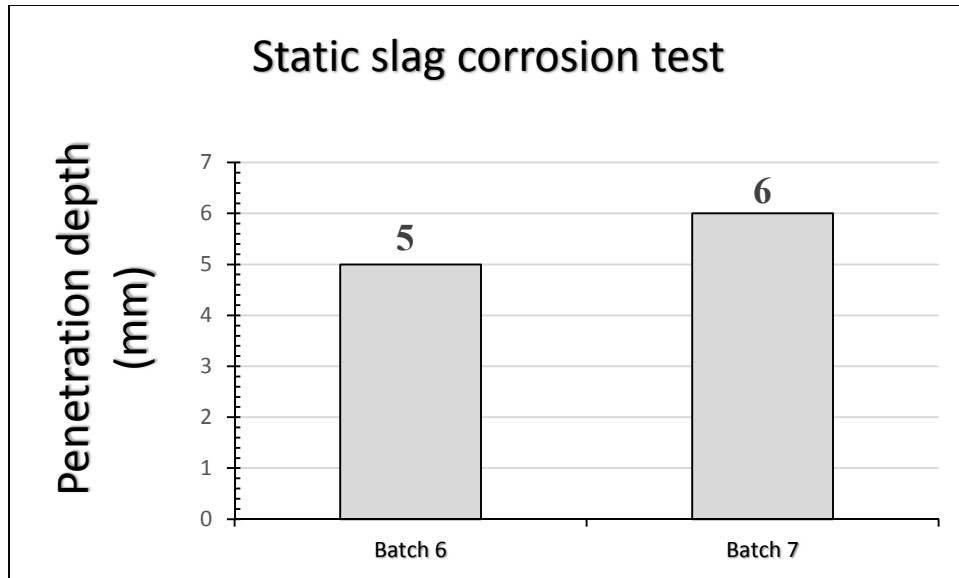


Fig.7.11: Graph of penetration depth of Static slag corrosion test with the different –different alumina fines

Fig.7.11 shows corrosion (mm) as a function of the variation of different–different alumina fines ASC refractories. It is clearly indicated that the corrosion of batch 7 sample is more than the batch 6. It is due to the size and surface area of reactive alumina.

Chapter – 8

Results & Discussion-IV Effect of antioxidant type on ASC Refractories

In this chapter the effect of different antioxidant (Al and Si metal powder) on various properties is explored. All of the experimental procedures was done as detailed in the previous section. With regards to change in composition investigated here, according to table 4.8. In this section, we compare batch 3(which had 2% Al metal powder) with batch 8(which had 1% Al and 1% Si metal powder).

8.1 Physical properties (before coking):

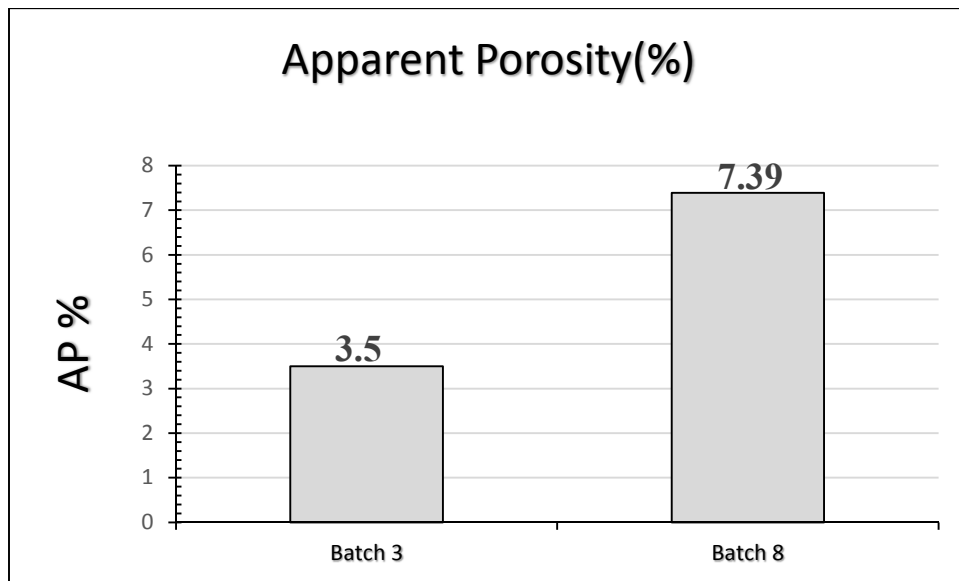


Fig.8.1: Variation of apparent porosity with the different antioxidant type

The change in AP with the different antioxidants is shown in fig.8.1. The AP value is more for batch 8 as compare to batch 3. This increase in porosity may arise due to the variation of manufacturing condition like mixing and pressing. The variation of bulk density is shown in fig.8.2. The bulk density appeared not to change very much. It is difficult to differentiate between 3.1 and 3.07. The variation of cold crushing strength is shown in fig. 8.3. The CCS value also decreases for batch 8. In the case of batch 8 there is improper filling of pores due to

which CCS value is decreased. The distribution of the resin around the aggregates may also be are the reason for decrease in strength.

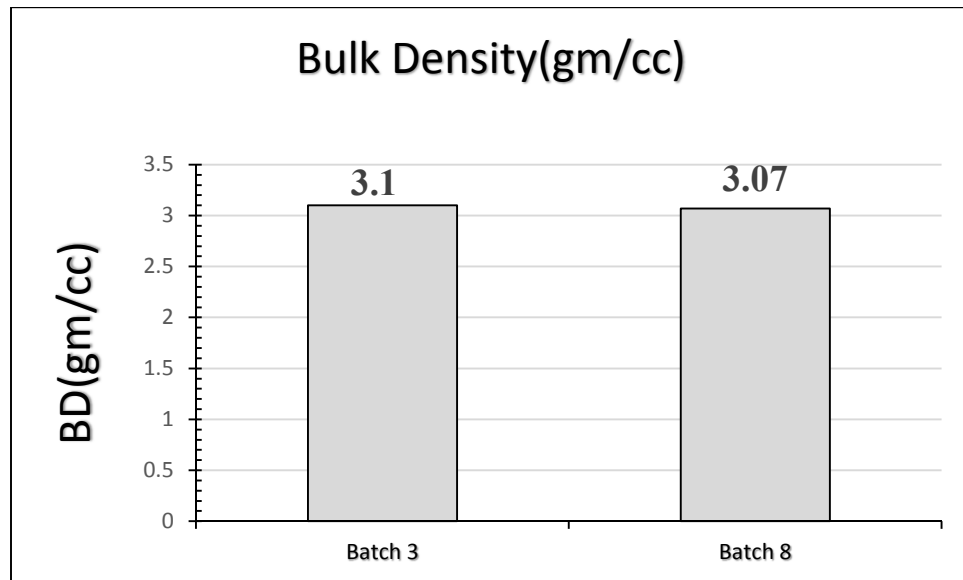


Fig.8.2: Variation of Bulk density with the different antioxidant type

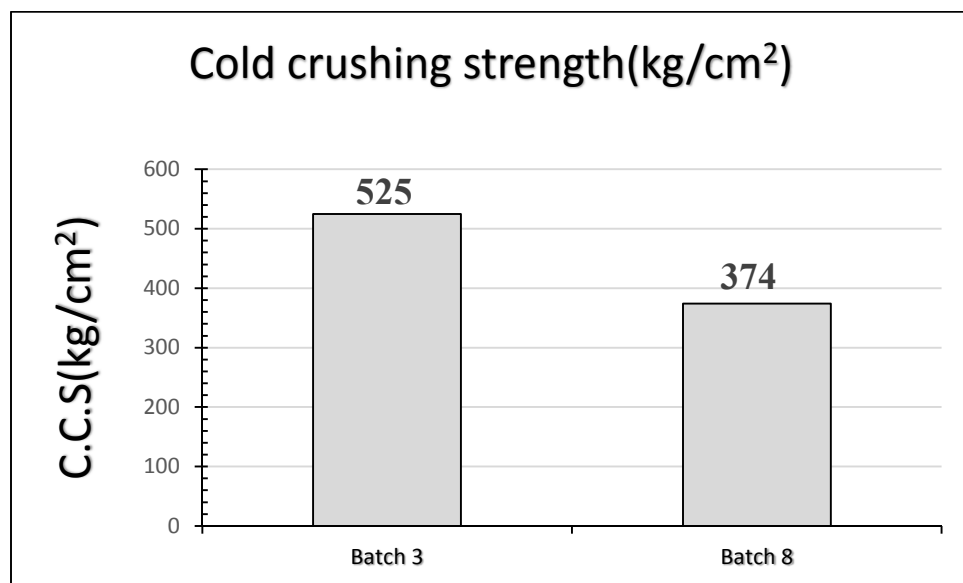


Fig.8.3: Variation of Cold crushing strength with the different antioxidant type

8. 2Physical properties (after coking):

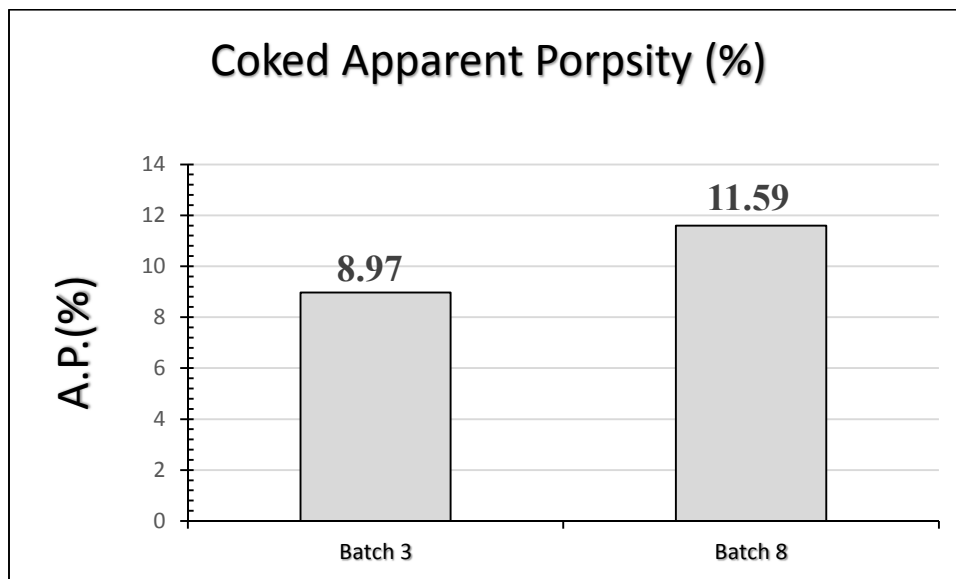


Fig.8.4: Variation apparent porosity of with the different antioxidant type

The change in coked AP with the different antioxidant type ratio is shown in fig.8.4. With the change of antioxidant the percentage of AP is increasing for batch 8. The coked bulk density (Fig.8.5) also follows a similar trend in that the BD for batch 8 decreases slightly to 3.03 gm/cc. The variation of coked cold crushing strength is shown in fig. 8.6. The CCS value is also slightly decreased of batch 8. The coked cold crushing strength appeared not to change very much, it is difficult differentiate between 316 and 305.

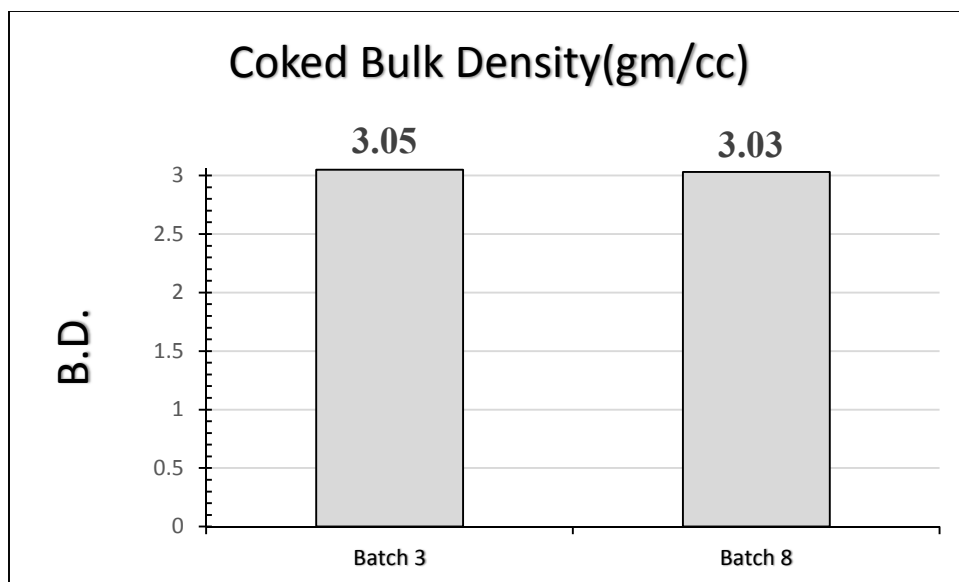


Fig.8.5: Variation of Bulk density with the different antioxidant type

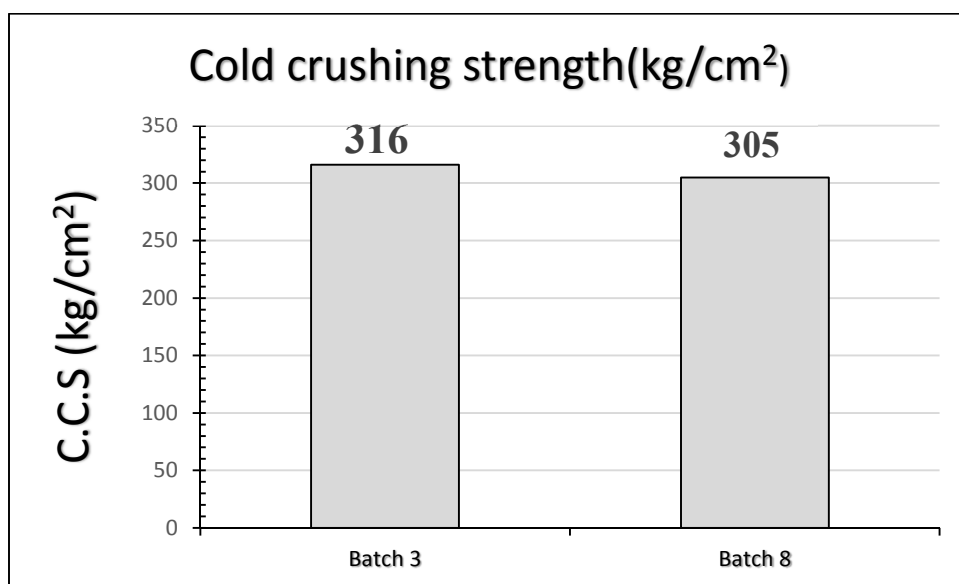


Fig.8.6: Variation of Cold crushing strength with the different antioxidant type

8.3 Thermal shock resistance:



Fig.8.7: Samples after 14th cycle

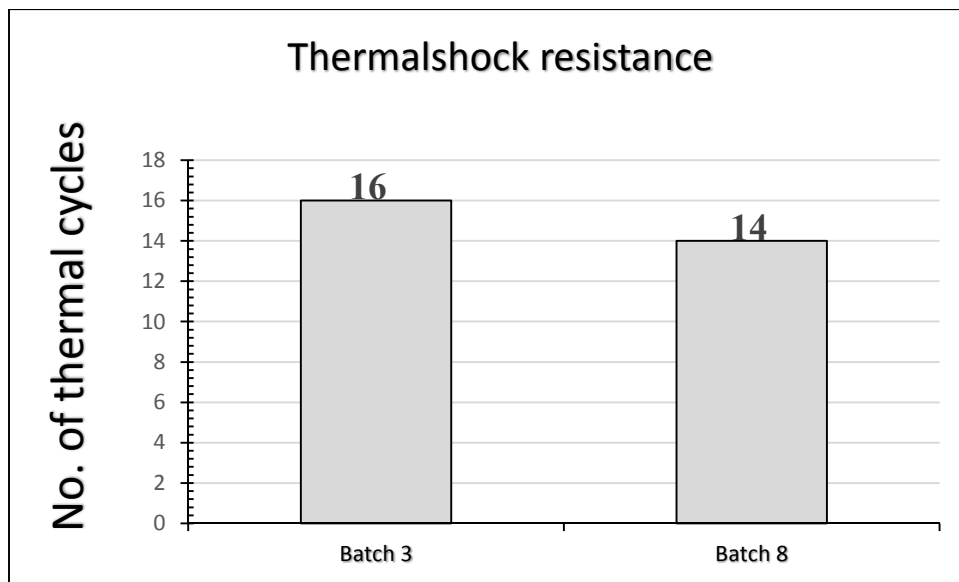


Fig.8.8: Graph of thermal shock resistance with the different antioxidant type

The thermal shock resistance of samples 3 and 8 are shown in the above figures. In batch 8 value of thermal shock is decreased may be because formation of SiC fibers, aluminum nitrides and aluminum carbides are less in comparison to the batch 3.

8.4 Oxidation resistance:



Fig.8.9: Images of the cross-section of the ASC specimens of Batch 8 oxidized at 1400°C for 10 hours

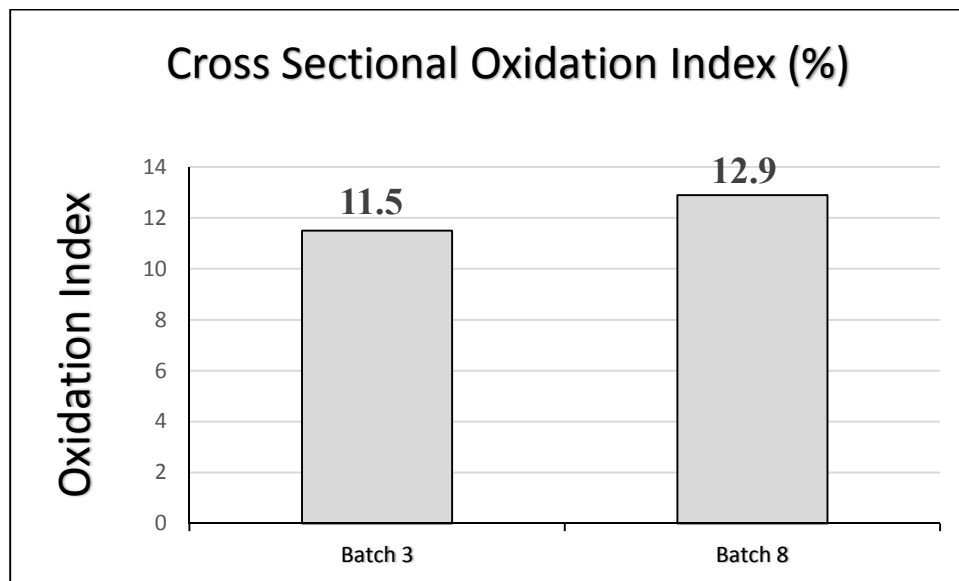


Fig. 8.10: Oxidation Index (%) of tempered ASC Batch 3 and Batch 8 samples oxidized at 1400 °C for 10hours with the different antioxidant type

The variation of the oxidation index of the ASC samples with the variation of different antioxidant type is presented in Fig.8.9 and 8.10. Oxidation image of batch 3 sample is given in Fig. 5.21. Interestingly, we have observed that there is practically not much difference in the oxidation behavior of the batch 8 samples (Fig 8.9) as compared to there of batch 3 samples (Fig 5.21). Even after geometrically calculating the oxidation area as well as the oxidation index for the samples are 11.5 and 12.9%, for batch 3 and 8 respectively. These values are close to each other.

8.5 Corrosion resistance:



Fig.8.11: Corroded sample of Batch 8 after cutting

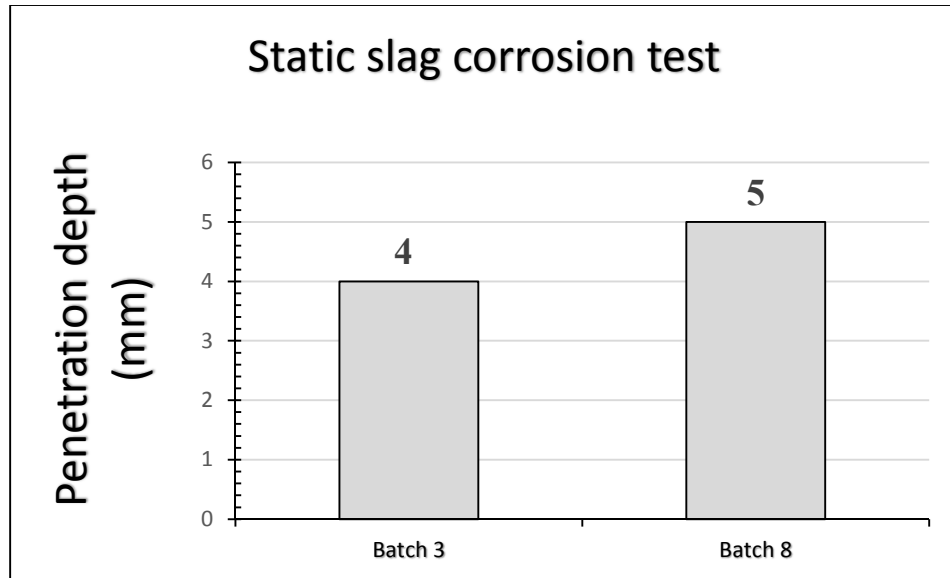


Fig.8.12: Graph of penetration depth of Static slag corrosion test with the different antioxidant type

Fig.8.12 shows corrosion (mm) as a function of the different antioxidant type ASC refractories. It is clearly indicated that the corrosion of batch 8 sample is slightly more than the batch 3. These values are similar to each other.

Chapter – 9

Summary and Conclusions

Al_2O_3 -SiC-C refractory is one of the most important refractories in the steel industry. Al_2O_3 -SiC-C bricks have many advantages over the Al_2O_3 -C brick lining.

An attempt has been made to reduce the graphite content of the Al_2O_3 -SiC-C refractory by replacing a percentage of the graphite by specially treated graphite in this study. Effect of addition of STG has been studied in this present work. Total carbon content used for these bricks were 7.5 wt%. Graphite was partially replaced by STG in the range of 0% to 2 wt%. Other raw materials used for this study were fused alumina, tabular alumina, antioxidants (Al and Si metal powder) and resin binder (both liquid and powder). The compositions were mixed and pressed and then characterized for various properties of both tempered and coked samples. The effect of STG was studied by different characteristics of the bricks and the properties were compared with the base brick which contained no STG under similar manufacturing conditions.

The significant features of the fabricated refractory are as follows.

1. The STG fortified Al_2O_3 -SiC-C refractories exhibited lower apparent porosity for 1.5 wt. % STG.
2. Apparent porosity of the coked samples shows progressive lowering in porosity with the amount of STG used. Additionally the coked bulk density was found to increase than the standard composition.
3. The trend of CCS for coked samples were similar to those of uncoked samples with the new composition showing ~20% increase in coked CCS.
4. The new composition exhibited remarkable increase in HMOR. The increment was almost 80% higher than that of the standard Al_2O_3 -SiC-C refractory.

5. The new formulations showed excellent thermal shock resistance. While the standard brick failed at 12 air quenching cycles, our composition went past 16 cycles.
6. Dramatic increase in oxidation resistance was observed for the new compositions with an index of ~11% as compared to ~30% for the standard composition.
7. The corrosion resistance of 1.5% STG fortified brick shows better corrosion resistance as compared to other compositions. But corrosion resistance is higher for without any STG content or standard composition of Al_2O_3 -SiC-C refractory.

In totally we have formulated a low carbon Al_2O_3 -SiC-C refractory with 7.5% graphite with special carbon additives that exhibits excellent thermo-mechanical properties as noted above. The compositions with 1.75 in batch 4 and 2 wt% in batch 5, STG additives had either comparable or inferior properties as compared to the standard composition. On the other hand, refractories with 1.5 in batch 3 and 1 wt% in batch 2, additives exhibited dramatically improved thermo-mechanical properties including slag corrosion resistance, thermal shock resistance and oxidation resistance but also in batch 6 and batch 8 is almost showed the comparable result with respect to batch 3, here also it include that the oxidation and slag corrosion resistance of batch 7 was almost inferior with respect to batch 3.

The technology demonstrated in this work is genetic to carbon/graphite containing refractories in that many of these classes of refractories can be strengthened with this approach. This work open up with a great opportunities to explore new and improved refractory systems for the future work.

Scope of future work:

This investigation has opened up with a fabulous scope of further research in this direction. The results so far obtained are highly inspiring and may lead to detailed scientific studies. Field trials should be carried out with this club of Al_2O_3 -SiC-C bricks in industrial operational condition. However, the positive effect of addition of specially treated graphite in Al_2O_3 -SiC-C refractory has been well-established in this study. A huge potential exists for commercial applications of this study to improve the properties of Al_2O_3 -SiC-C refractories in future.

REFERENCES:

1. Annual book of ASTM standard, Refractories: Activated carbon, Activated ceramics, 15.01, pp. 19 (2003).
2. Emad.Mohamed M.Ewais, Carbon based refractories, Journal of the Ceramic Society of Japan, 112[10]2004, 517-532.
3. <http://www.indiasteelexpo.in/IndustryOverview.php>
4. O. Sasan, D.Arash, Micro structure and phase evolution of alumina-spinel self-flowing refractory castables containing nano-alumina particles, CeramicsInternational37(2011)1003–1009.
5. G.D.T. Angeles, J.V.Francisco, H.D.A.Antonio, Direct mineralogical composition of a MgO–C refractory material obtained by Rietveld methodology, Journal of The European Ceramic Society26 (2006) 2587–2592.
6. X. C. Li, B.Q. Zhu, T.X. Wang, Effect of electromagnetic field on slag corrosion resistance of low carbon MgO–C refractories, Ceramics International38(2012)2105–2109.
7. P. Nicolas, O. Evariste, High temperature mechanical characterization of an alumina refractory concrete for blast furnace main trough Part I. General context, Journal of The European Ceramic Society28(2008) 2859–2865.
8. W.S. Resende, R.M. Stoll, S.M. Justus ,R.M. Andrade ,E. Longo, J.B. Baldo, E.R. Leite, C.A. Paskocimas, L.E.B. Soledade, J.E.Gomes, J.A. Varela, Key features of alumina/magnesia/graphite refractories for steel ladlelining, Journal of The European Ceramic Society20(2000) 1419–1427.
9. S. Mucahit, A. Sedat, O. Salih, A micro structural study of surface hydration on a magnesia refractory, Ceramics International36(2010) 1731–1735.

10. O. Sasan, A.B. Mohammad, M. Fatollah, M. Fatollah, R.N. Mohammad, The effect of de flocculants on the self-flow characteristics of ultra-low-cement castables in Al₂O₃–SiC–C system, *Ceramics International* 31 (2005) 647–653.
11. C.G. Aneziris, U. Klippel, W. Schärfl, V. Stein, Y.W. Li, *Int. J. Appl. Ceram. Technol.* 4 (6) (2007) 489–1489.
12. C.G. Aneziris, D. Borzov, J. Ulbricht, *Interceram* (2003) 22–27.
13. E. Mohamed, M. Ewais, *J. Ceram. Soc. Jpn.* 112 (10) (2004) 517–532.
14. C.F. Cooper, I.C. Alexander, C.J. Hampson, *Br. Ceram. Trans. J.* 84 (2) (1985) 57–62.
15. M.N. Khezrabadi, J. Javadpour, H.R. Rezaie, R. Naghizadeh, *J. Mater. Sci.* 41 (2006) 3027–3032.
16. S. Zhang, N.J. Marriott, W.E. Lee, *J. Eur. Ceram. Soc.* 21 (2001) 1037–1047.
17. B. Liu, Y.F. Liu, K.Q. Liu, J.L. Sun, *Naihuo Cailiao* 44 (2) (2010) 123–125
18. Hand book of refractories
19. S. Tamura, T. Ochiai, S. Takanaga, T. Kanai, H. Nakamura, Nano- tech. refractories-1: the development of the nano structural matrix, in: *Proceedings of the UNITECR'03 Congress, Osaka, Japan, 19–22 October, 2003*, pp.517–520.
20. S. Takanaga, T. Ochiai, S. Tamura, T. Kanai, H. Nakamura, Nano- tech. refractories-2: the application of the nano structural matrix to MgO–C bricks, in: *Proceedings of the UNITECR'03 Congress, Osaka, Japan, 19–22 October, 2003*, pp.521–524.
21. S. Takanaga, Y. Fujiwara, M. Hatta, T. Ochiai, S. Tamura, Nano- tech. refractories 3: development of “MgO-rimmed MgO–Cbrick”, in *Proceedings of the UNITECR'05 Congress, Orlando, USA, 8–11 November, 2005*.

22. Y. Shiratani, T. Yotabun, K. Chihara, T. Ochiai, S. Tamura, Nano- tech. refractories-4: the application of the nano structural matrix to SN plates, in: Proceedings of the UNITECR'05 Congress, Orlando, USA, 8–11 November, 2005.
23. M. Hatta, S. Takanaga, O. Matsuura, T. Ochiai, S. Tamura, Nano- tech. refractories-5: the application of B₄C–C nano particles to MgO–C bricks, in: Proceedings of the UNITECR'07 Congress, Dresden, Germany, 18–21 September, 2007, p. 614.
24. S. Tamura, Y. Urushibara, O. Matsuura, T. Shin, Nano-tech. refractories-6: observation of the texture after carbonization of nano-tech refractories, in: Proceedings of the UNITECR'07 Congress, Dresden, Germany, 18–21 September, 2007, p. 627.
25. H. Hattanda, T. Yotabun, T. Tsuda, T. Ochiai, S. Tamura, Nano-tech. refractories-7: application of nano structured matrix to SN plates, in: Proceedings of the UNITECR'07 Congress, Dresden, Germany, 18–21 September, 2007, pp. 204–207.
26. S. Tamura, T. Ochiai, S. Takanaga, T. Kanai, H. Nakamura, Nano- tech. refractories-8: technological philosophy and evolution of nano- tech. refractories, in: Proceedings of the UNITECR'11 Congress, Kyoto, Japan, October 30–November 2, 2011.
27. H. Yasumitsu, M. Hirashima, O. Matsuura, S. Takanaga, T. Ochiai, S. Tamura, Nano-tech. refractories-9: the basic study on the formation of the nano structured matrix in MgO–C bricks, in: Proceedings of the UNITECR'11 Congress, Kyoto, Japan, October 30–November 2, 2011.
28. M. Tanaka, H. Kamioa, J. Yoshitomi, T. Kayama, S. Hanagiri, K. Goto, Nano-tech. refractories-10: nano-tech. MgO–C bricks for converters to minimize the heat loss, in: Proceedings of the UNITECR'11 Congress, Kyoto, Japan, October 30–November 2, 2011.

29. H. Hattanda, T. Yotabun, T. Tsuda, H. Tanabe, Nano-tech. refractories- 11: the application of nano-technology to AG material for SN plates and carbon bricks for blast furnaces, in: Proceedings of the UNITECR'11 Congress, Kyoto, Japan, October 30–November 2, 2011.
30. M. Bag, S. Adak, R. Sarkar, Study on low carbon containing MgO–C refractory: use of nano carbon, *Ceramics International* 38 (2012) 2339–2346.
31. M. M. J. Treacy, T. W. Ebbesen, J. M. Gibson, Exceptionally high Young's modulus observed for individual carbon nanotube, *Nature* 381 (1996) 678–680.
32. M. F. Yu, O. Lourie, M. J. Dyer, K. Moloni, T. F. Kelly, Strength and breaking mechanism of multi walled carbon nano tubes under tensile load, *Science* 287(2000) 637–640.
33. Y. Matsuo, M. Tanaka, J. Yoshitomi, S. Yoon, J. , Miyawaki, Effect of the carbon nano fiber addition the mechanical properties of MgO–C brick, : Proceedings of UNITECR'11 Congress, October 30–November 2, Kyoto, Japan , 2011.
34. M. Luo, Y. Li, S. Jin, S. Sang, L. Zhao, Y. Li, Micro structures and mechanical properties of Al₂O₃–C refractories with addition of multi- walled carbon nano tubes, *Materials Science and Engineering A* 548 (2012) 134–141.
35. V. Roungos, C. G. Aneziris, Improved thermal shock performance of Al₂O₃–C refractories due to nano scaled additives, *Ceramics International* 38 (2012) 919–927.
36. B. Z. Jang, A. Zhamu, Processing of nano grapheme platelets (NGPs) and NGP nano composites: a review, *Journal of Materials Science* 43 (2008) 5092–5101.
37. J. R. Potts, D. R. Dreyer, C. W. Bielawski, R. S. Ruoff, Graphene- based polymer nano composites, *Polymer* 52 (2011) 5–25.

38. R. Sengupta, M. Bhattacharya, S. Bandyopadhyay, A. K. Bhowmick, A review on the mechanical and electrical properties of graphite and modified graphite reinforced polymer composites, *Progress in Polymer Science* 36 (2011) 638–670.
39. Y. Fan, L. J. Wang, J. L. Li, S. K. Sun, F. Chen, L. D. Chen, W. Jiang, Preparation and electrical properties of graphene nano sheet/ Al_2O_3 composites, *Carbon* 48 (2010) 1743–1749.
40. P. Kun, O. Tapasztó, F. Weber, C. Balazsi, Determination of structural and mechanical properties of multi-layer graphene added silicon nitride-based composites, *Ceramics International* 38 (2012) 211–216.
41. K. Wang, Y. F. Wang, Z. J. Fan, J. Yan, T. Wei, Preparation of graphene nano sheet/alumina composites by spark plasma sintering, *Materials Research Bulletin* 46 (2011) 315–318.
42. Ewais, E.M.M., “Carbon based refractories”, *J. Ceram. Soc. Jpn.*, 112, pp.517-532(2004).
43. Qeintela, MA., Santos, FD., Pessoa CA., Rodrigues, JA., and Pandolfelli, VC., “ MgO-C refractories for steel ladles slag line”, *Refractories Applications and news*, 11, pp.15-19 (2006).
44. S.N.Silva, O.R. Marques, P.A. Peixoto, C.A. Pascocimas, E.Longo and J.A.Varela, “Slag Attack in High Alumina Refractory used in Torpedo Car”, *UNITECR – 93*, P – 1365.
45. J.R.C Filho, M.P.Bastos and G.C. Filho, “Performance of $\text{Al}_2\text{O}_3 - \text{SiC} - \text{C}$ for Torpedo Car Lining”, *UNITECR – 93*, P – 1353
46. Y. Kubo, K.Doura, J. Yagi and N. Hiroki, “Improvement of Refractory for Torpedo Ladle with Hot Metal Pretreatment”, *UNITECR – 93*, P – 1354

47. Publication type, Application. Application number, CN 201310000610. Publication date, Apr 3, 2013. Filing date, Jan 4, 2013. Priority date, Jan 4, 2013.
48. M. Mishima, T. Hokii and K. Asano, “Influence of Carbon Content on the Thermal Properties of $\text{Al}_2\text{O}_3 - \text{SiC} - \text{C}$ Brick for Torpedo Cars”, Journal of Technical Association of Refractories, Japan, Vol 30, No. 1, March, 2010, P 42 – 45.
49. S. M. Justus, “Post Mortem Study of $\text{Al}_2\text{O}_3/\text{SiC}/\text{C}/\text{MgAl}_2\text{O}_4$ Ceramic Lining used in Torpedo Cars”, Ceramic International, 31, 2005, P 897 – 904.
50. K. Nakanishi, “Improvement of the Torpedo Car Lining Refractories for Resource Recycling”, UNITECR 03.
51. P. Jeschke and G. Mortl, “Recent Trends in Refractories for Iron and Steel Production”, UNITECR – 93
52. W. Zhanmin, W. Qiang and C. Xiying, “ effect of Al Addition on Properties of $\text{Al}_2\text{O}_3 - \text{SiC} - \text{C}$ Dry Ramming Mixes for BF Trough”, China’s Refractories, Vol. 17, No. 3, July-Sept, 2008.
53. Liu Guoki, Li Hongxia, Yang Bin and Yang Jinsong, “Effect of Composite Metal Additives on Properties of $\text{Al}_2\text{O}_3 - \text{Graphite}$ Composites”, UNITECR – 07, P – 82.
54. Fan H., Li Y., & Sang S., 2011. Microstructures and mechanical properties of $\text{Al}_2\text{O}_3\text{-C}$ refractories with silicon additive using different carbon sources. Materials Science and Engineering A, 528, pp.3177–3185.
55. Amin M.H., Amin-Ebrahimabadi M. & Rahimipour M., 2009. The effect of nanosized carbon black on the physical and thermomechanical properties of $\text{Al}_2\text{O}_3\text{-SiC-SiO}_2\text{-C}$ composite. Journal of Nanomaterials, 2009, Article ID 325674, doi:10.1155/2009/325674

56. BosallSB, HenryDK. Am Ceram Soc 1985; **13:331–40**.
57. ChanC, ArgentBB, LeeWE. J AmCeramSoc 1998; **81(12):3177–88**.
58. V. Rongos and C.G. Aneziris Department of Ceramic, Glass and Construction Materials, TU Bergakademie Freiberg, Agricolastraße 17, 09596 Freiberg, Germany Received 30 May 2011; received in revised form 2 August 2011; accepted 4 August 2011 Available online 11 August 2011
59. Tamura S., Ochiai T., Takanaga S., Kanai T. & Nakamura H., 2003. Nano-Tech Refractories – 1. The Development of the Nano Structural Matrix, paper presented at the Unified International Technical Conference on Refractories, Kyoto, Japan: UNITECR'03, Papers 517-520.
60. Kido N., Yamamoto K., Kamiide M., Fuchimoto H., Suruga T., Hoki T. & Asano K. 2003. Carbon Nanofiber - A New Trial for Magnesite Based Bricks, paper presented at the Unified International Technical Conference on Refractories, Kyoto, Japan: UNITECR'03, Papers 264-267.
61. B. Liu, Y. Liu, K. Liu, and J. Sun: Naihuo Cailiao **44**[2] 123-125 (2001)
62. J. Zhang, J. Jeong, J. Lee, C. Won, D. Kim: Mater. Res. Bull., **37** 319-329 (2002)
63. T. Ebadzadeh, M. Heidarzadeh-Tari an Falamaki: Adv. Appl. Ceram., **108**[6] 369-372 (2009)
64. B. Pavel, G. Dmitry, G. Alexander, V. Pavel and A. Leonid: J. Nanosci. Nanotechno., **10**[8] 4992-4997 (2010) .
65. V. Garnier, G. Fantozzi, D. Nguyen, J. Dubois and G. Thollet: J. Eur. Ceram. Soc., **25** 3485-3493 (2005)

66. Ming Luo, Yawei Li , Shengli Jin, Shaobai Sang and Lei Zhao, Yuanbing Li
 “Microstructures and mechanical properties of Al₂O₃-C with addition of multi walled carbon nano tubes” Received 24 August 2011 Received in revised form 8 February 2012
 Accepted 1 April 2012 Available online 7 April 2012
67. Heng Wang, Yawei Lin, Tianbin Zhu, Shaobai Sang and Qinghu Wang “Micro structures and mechanical properties of Al₂O₃-C refractories with addition of micro crystalline graphite”
 Received 13 March 2014; accepted 25 March 2014
68. Qinghu Wang, Yawei Lin, Ming Luo, Shaobai Sang, Tianbin Zhu and Lei Zhao
 “Strengthening mechanism of graphene oxide nano sheets for Al₂O₃-C refractories”
 Received 24 February 2013; received in revised form 29 May 2013; accepted 29 May 2013
69. Buchel, G. *et al.* Review of Tabular Alumina as higher performance Refractory Material, Interceram (2007), pp (6-12)
70. Kriechbaum, G. W. *et al.* Review on the properties and application of tabular alumina in refractories.
71. Shaw, K., “Carbon and graphite,” Hand book of refractories and their uses, applied science Publisher Ltd., London (1972) pp. 140-145.
72. Cooper, C. F., Refract J. Vol. 6 (1980).
73. Russell, F. S., Refract J. Vol. 6 pp. 7-10 (1982).
74. Cooper, C. F., Chem. Ind., Vol. 18, pp. 678-429 (1972).
75. Nishimura, D., “Technical trends of phenolic for Japanese refractories”, Taikabutsu Overseas, 15, pp. 10-14 (1995).

76. J. R. O'CONNOR and J. SMILTENS (Eds.), Silicon Carbide: A High Temperature Semiconductor, (Proc. Conf. on Silicon Carbide, Boston, Mass.) Pergamon Press, New York (1960).
77. Wen-ShyongKuo, Tsung-Lin Wu, Hsin-Fang Lu and Tzu-Sen Lo "Microstructure and mechanical properties of nano-flake graphite composites", 16th International conference on composite materials, Kyoto, Japan (2007).
78. Zhang Shengtao, GuAnyan, GaoHuanfang and CheXiangqian "Characterization of Exfoliated Graphite Prepared with the Method of Secondary Intervening" International Journal of Industrial Chemistry", (2011).
79. Eduardo H.L. Falcao, Richard G. Blair, Julia J. Mack, Lisa M. Viculis, Chai-Won Kwon, Michael Bendikov, Richard B. Kaner, Bruce S. Dunn and Fred Wudl, "Microwave exfoliation of a graphite intercalation compound", Carbon 45 (2007) 1364–1369.
80. Yoshida A., Hishiyama Y., Inagami M., "Exfoliated graphites from various intercalation compounds", Carbon Vol. 29. No. 8. pp. 1227-1231. 1991.
81. BeataTryba, Antoni W. Morawski, Michio Inagaki, "Preparation of exfoliated graphite by microwave irradiation", Carbon 43 (2005) 2397–2429.
82. Tong Wei, Zhuangjun Fan, GuilianLuo, Chao Zheng, DashouXie, "A rapid and efficient method to prepare exfoliated graphite by microwave irradiation", Carbon 47 (2008) 313–347.
83. SHAW K., Refractories and Their Uses, Applied Science Publishers Ltd., London, 1972.
84. CHANDLER H. W., Thermal Shock of Refractories, Proc. Tehran Int. Conf. of Refractories, 2004, 28–39.
85. American Society of Testing and Materials Standards, Sect. 15, Vol. 15.01, 1990.

86. British Standard Testing of Engineering Ceramics, BS 7134, Section 1.2, 1989.
87. Mineral Aggregate Conservation Reuse and Recycling. Report prepared by John Emery
Geotechnical Engineering Limited for Aggregate and Petroleum Resources Section,
Ontario Ministry of Natural Resources. Ontario, 1992.